SELF-ORGANIZED CRITICALITY AND THE DEVELOPMENT OF EEG PHASE RESET

Thatcher, R.W. [1,2], North, D.M.[2], and Biver, C. J.[2]

Department of Neurology, University of South Florida College of Medicine, Tampa, Fl.[1] and EEG and NeuroImaging Laboratory, Applied Neuroscience, Inc., St. Petersburg, Fl[2]

Send Reprint Requests To:
Robert W. Thatcher, Ph.D.
NeuroImaging Laboratory
Applied Neuroscience, Inc.
St. Petersburg, Florida 33722
(727) 244-0240, rwthatcher@yahoo.com

ABSTRACT

Objectives: The purpose of this study was to explore human development of self-organized criticality as measured by EEG phase reset from infancy to 16 years of age.

Methods: The electroencephalogram (EEG) was recorded from 19 scalp locations from 458 subjects ranging in age from 2 months to 16.67 years. Complex demodulation was used to compute instantaneous phase differences between pairs of electrodes and the 1st & 2nd derivatives were used to detect the sudden onset and offset times of a phase shift followed by an extended period of phase locking. Mean phase shift duration and phase locking intervals were computed for two symmetrical electrode arrays in the posterior-to-anterior locations and the anterior-to-posterior directions in the alpha frequency band (8 – 13 Hz).

Results: Log-log spectral plots demonstrated $1/f^{\alpha}$ distributions ($\alpha \approx 1$) with longer slopes during periods of phase shifting than during periods of phase locking. The mean duration of phase locking (150 – 450 msec) and phase shift (45 – 67 msec) generally increased as a function of age. The mean duration of phase shift declined over age in the local frontal regions but increased in distant electrode pairs. Oscillations and growth spurts from mean age 0.4 years to 16 years were consistently present.

Conclusions: The development of increased phase locking in local systems is paralleled by lengthened periods of unstable phase in distant connections. Development of the number and/or density of synaptic connections is a likely order parameter to explain oscillations and growth spurts in self-organized criticality during human brain maturation.

Key Words: Development of EEG phase reset, phase locking, chaos, self-organizational criticality.

1.0- Introduction

Understanding the mechanisms of neural synchronization and desynchronization is important in understanding human brain dynamics. Recent studies have shown that sudden transitions in the amplitude of the human electroencephalogram (EEG) are represented by power laws and scale invariance and long-range temporal correlations (Freeman 2003; Nikulin and Brismar, 2005; Linkenkaer-Hansen et al, 2001; Parish et al, 2004). These studies are important because long-range temporal correlations are a reliable method to transfer information in neuronal populations as well as providing a linkage to general laws of physics of complex systems (Bak et al, 1987; 1988; Chialvo and Bak, 1999; Beggs and Plenz, 2003; Rios and Zang, 1999). The rapid creation and destruction of multistable spatial-temporal patterns have been evaluated in evoked, transient and spontaneous EEG studies (Breakspear and Terry, 2002a, 2002b; Rudrauf et al, 2006; Le Van Quyen, 2003). The patterns of spontaneously occurring synchronous activity involve the creation of differentiated and coherent neural assemblies at local, regional and large scales (Breakspear and Terry, 2002a; 2002b; Rudrauf et al, 2006; Stam and de Bruin, 2004; Varela, 1995; Freeman and Rogers, 2002). The dynamic balance between synchronization and desynchronization is considered essential for normal brain function and abnormal balance is often associated with pathological conditions such as epilepsy (Lopes da Silva and Pihn, 1995; LeVan Quyen et al, 2001b; Chevez et al, 2003; Netoff and Schiff, 2002), schizophrenia (Lere et al., 2002) and dementia (Stam et al., 2002a; 2002b).

Synchronization is commonly defined as an "adjustment of rhythms of oscillating objects due to their weak interaction" and nearly always involves a period of stable phase relations or phase locking (Pikovsky et al, 2003). De-synchronization is the opposite of synchronization and is defined as a shift in the phase difference of synchronized oscillators and elimination of phase locking. Notice that both synchronization and de-synchronization start with a phase shift or adjustment but differ in the absence or extent of phase locking. Phase locking is a tell tale sign of synchronization and this is why Freeman and colleaques (Freeman, 2003; Freeman and Rogers, 2002) and Blackstone and Williams (2004) and others (Lachaux et al, 2000; LeVan Quyen et al, 2001b) use phase locking as a measure of EEG synchronization.

The study of rapid changes in phase difference followed by periods of phase locking is called "Phase Reset" (PR). Phase reset occurs in coupled nonlinear oscillators when there is a sudden shift of the phase relationship of oscillators to a new value followed by a period of phase locking or phase stability also called phase synchronization (Pikovsky et al, 2003). The term phase synchrony is

synonymous with phase locking and is sometimes preferred in order to emphasize the statistical nature of phase stability (Rudrauf et al, 2006). However, the term phase synchrony is often used in reference to EEG coherence whereas phase locking is more specific to phase reset. Whether one refers to phase locking or phase synchrony what is important in the measurement of phase reset is that there is a prolonged period of phase stability following a phase shift. This is important because random phase shifts without stability exhibit "white noise" distributions (Pikovsky et al, 2003; Tass, 1997). Phase reset is also important because it results in increased EEG amplitudes due to increased phase locking of synaptic generators (Cooper et al, 1965; Nunez, 1994; Lopes da Silva, 1994). The integrated rapid sequencing of phase shifts followed by phase locking (i.e., the two fundamental components of phase reset) have been correlated to the alpha frequency band during cognitive tasks (Kahana; 2006; Kirschfeld, 2005; Tesche and Karhu, 2000; Jensen and Lisman, 1998),working memory (John, 1968; Rizzuto et al, 2003; Damasio, 1989; Tallon-Baudry et al, 2001), sensory-motor interactions (Vaadia et al, 1995; Roelfsema et al, 1997), hippocampal long-term potentiation (McCartney et al, 2004) and consciousness (Cosmelli et al, 2004; Varela et al, 2001; John, 2002; 2005). The present study builds on these previous studies by parametrically analyzing the maturation of the two fundamental components of phase reset: 1- phase shift followed by, 2- phase stability in a large population of subjects from infancy to adolescence.

There are two general and equivalent methods for studying phase reset: 1- narrow band decomposition and, 2- broad band decomposition (Rudrauf et al, 2006; Le Van Quyen et al, 2001a; Bruns, 2004). Both methods use analytic transforms such as the Fourier transform, Wavelet transform and Hilbert transform. Which method is used depends on the frequency resolution desired and the nature of the transient signals that are to be detected (Rudrauf et al, 2006;Tass, 1997; Le Van Quyen et al, 2001a; Lachaux et al, 2000; Freeman et al, 2003; 2006; Freeman and Rogers, 2002). In the present paper we used complex demodulation as an analytic signal processing method similar to Lachaux et al (2000) and Blackstone and Williams (2004) which is mathematically the same as the Hilbert transform (Pikovsky et al, 2003; Oppenheim and Schafer, 1975). All methods measure the phase difference of pairs of signals evaluated over successive intervals of time where phase stability is when the first derivative approximates zero or $d\varphi_{i,j}/dt \approx 0$. In general, the magnitude of phase shift is defined as the difference between the pre-phase shift value minus the post-phase shift value and if a sudden and significant phase difference occurs followed by an extended period of phase stability then the point in time when the phase shift started is the time when the first derivative exceeded some threshold value

(Rudrauf et al, 2006; Tass, 1997; Tass et al, 1998; Le Van Quyen et al, 2001a; Blackstone and Williams, 2004). This point in time marks the onset of phase reset. EEG phase shift offset is defined in a reverse manner and the onset and offset times define the phase shift duration. The phase shift duration is typically in the range of 20 msec to 80 msec (Buzaski, 2006; Freeman, 2003; Freeman and Rogers, 2002). Phase locking or phase stability that follows a phase shift is often 200 msec to 600 msec in duration in single cell analyses (Gray et al, 1989) and 100 msec to 1 second in surface recordings (Freeman and Baird; 1987; Freeman and Rogers, 2002; Freeman et al, 2006; Blackstone and Williams, 2004).

Recently, Linkenkaer-Hansen et al (2001); Stam and de Bruin (2004); Blackstone and Williams, 2004; Freeman et al (2003; 2006) and Buzaski (2006) have shown that the EEG spectrum is best fit by a power function with a $1/f^{\alpha}$ distribution. The "one over f" distribution is shared by a very wide range of observations in the universe and was one of the intriguing mysteries in physics until Bak et al (1987) created a mathematical and computer model of the process of 1/f. Bak et al (1987) referred to their model as "self-organized criticality" (SOC) because of their discovery of the spontaneous emergence of minimal stability with spatial scaling that leads to a 1/f power law for temporal fluctuations. Many studies have subsequently replicated and extended the mathematics and physics of SOC models (Bak, 1996). An invariant feature of SOC is the presence of "activation-deactivation" processes and dissipation of energy which are fundamental to the 1/f distribution (Riuos and Zhang, 1999; Davidson and Schuster, 2000). The interplay of the dissipation and supply of energy from a source determines the amplitude and phase of all self-sustained nonlinear oscillators and activation-deactivation and dissipation are fundamental characteristics of neurons as well as most biological oscillators (Winfree, 1980; Pikovsky et al (2003).The link of SOC models to EEG requires a minimum of three factors: 1- measurement of an activation-deactivation process (e.g., rapid phase shift followed by stability), 2- an approximate 1/f distribution in a log-log plot and, 3- spatial scaling and temporal fluctuations where there are long-range spatial correlations (Bak et al, 1987; 1988; Bak, 1996; Davidson and Schuster, 2000). The analyses of Freeman et al (2003; 2006) and Blackstone and Williams (2004) demonstrated that the fine temporal structure of the EEG is characterized by 1/f distributions with periods of "unstable" phase dynamics followed by periods of "phase stability". These studies and others (Breakspear and Terry, 2002a; 2002b) indicate that the human EEG fundamentally exhibits characteristics of "self-organizational criticality", where sudden phase shifts are "unstable phase dynamics" and phase locking or "phase synchrony" is "phase stability". Furthermore, these studies

demonstrated that the terms "phase reset" and "SOC" when coupled with the 1/f distribution and activation-deactivation of self-sustaining nonlinear oscillators are synonymous terms in complex systems (Bak et al, 1987; 1988; Bak, 1996; Rios and Zang, 1999).

Currently there are no studies of the early childhood development of EEG phase reset. Nikulin and Brismar (2005) studied EEG age dependence of $1/f^{\alpha}$ distributions in 96 adult subjects. Interesting age and gender correlations were presented, however, phase shift duration and phase locking were not separately analyzed. Developmental changes in the number of phase resets per second and the duration of phase shifts and the length of phase locking are currently unknown and such information may be important in understanding the development of human neural dynamics. Therefore, the purpose of the present study is to investigate the development of human EEG phase reset from infancy to 16 years of age. The null hypotheses to be tested are: 1- there are no 1/f distributions of EEG phase reset, 2- there are no left and right hemispheric differences in the development of phase reset; 3- there are no differences in phase reset as a function of anterior-to-posterior vs. posterior-to-anterior direction, 4- there are no differences in phase reset as a function of inter-electrode distance, 5- there are no changes in phase reset as a function of age.

2.0 – Methods

2.1 Subjects

A total of 458 subjects ranging in age from 2 months to 16.67 years (males = 257) were included in this study. The subjects in the study were recruited using newspaper advertisements in rural and urban Maryland (Thatcher et al, 1987; 2003; 2007). The inclusion/exclusion criteria were no history of neurological disorders such as epilepsy, head injuries and reported normal development and successful school performance. None of the subjects had taken medication of any kind at least 24 hours before testing. All of the subjects were within the normal range of intelligence as measured by the WISC-R and were performing at grade level in reading, spelling and arithmetic as measured by the WRAT and none were classified as learning disabled nor were any of the school aged children in special education classes. All subjects ≥ 2 years of age were given an eight-item "laterality" test consisting of three tasks to determine eye dominance, two tasks to determine foot dominance, and three tasks to determine hand dominance. Scores ranged from – 8 (representing strong sinistral preference or left handedness), to +8 (representing strong dextral preference or right handedness). Dextral dominant children were defined as having a laterality score of ≥ 2 and sinistral dominant children were defined as having a laterality score of

≤ - 2. Only 9% of the subjects had laterality scores ≤ - 2 and 87% of the subjects had laterality scores ≥ 2 and thus the majority of subjects were right side dominant.

2.2 EEG Recording

Power spectral analyses were performed on 58 seconds to 2 minute 17 second segments of EEG recorded during resting eyes closed condition. The EEG was recorded from 19 scalp locations based on the International 10/20 system of electrode placement, using linked ears as a reference. The average reference and a Laplacian reference were not used because these reference methods involve mixing the amplitude and phase from different scalp locations resulting in phase and coherence distortions as shown by Rappelsberger (1989), Kamiński et al (1997) and Essl and Rappelsberger (1998). Eye movement electrodes were applied to monitor artifact and all EEG records were visually inspected and manually edited to remove any visible artifact. Each EEG record was plotted and visually examined and split-half reliability and test re-test reliability measures of the artifacted data were computed using the Neuroguide software program (NeuroGuide, v2.3.8). Split-half reliability tests were conducted on the edited EEG segments and only records with > 90% reliability were entered into the spectral analyses. The amplifier bandwidths were nominally 1.0 to 30 Hz, the outputs being 3 db down at these frequencies. The EEG was digitized at 100 Hz and up-sampled to 128 Hz and then spectral analyzed using complex demodulation (Granger and Hatanaka, 1964; Otnes and Enochson, 1978) (see section 2.3).

EEG phase differences and phase reset metrics was computed in the alpha frequency band (8.0 – 13.0 Hz) for anterior-to-posterior electrodes Fp1/2-F3/4; Fp1/2-C3/4; Fp1/2-P3/4 and Fp1/2-O1/2 and for posterior-to-anterior electrodes O1/2-P3/4; O1/2-C3/4; O1/2-F3/4 and O1/2-Fp1/2. This recording arrangement provides a stable matrix and test of spatial homogeneity by using five equally spaced electrodes per hemisphere with increasing distance between electrodes in the anterior-to-posterior and posterior-to-anterior directions. According to volume conduction there is a homogeneous decline of voltage as a function of distance from any source at near zero phase delay. The five equally spaced electrode locations is a direct test of volume conduction versus cortical connectivity (Thatcher et al, 1986; 1998). Factors used in the multivariate analysis of variance were: 1- Hemisphere, 2- Direction, 3- Inter-electrode distance and 4- Age. The analyses of different frequency bands demonstrated that the alpha frequency band exhibits the strongest developmental trends and therefore this study will focus exclusively on the 8 – 13 Hz alpha frequency band (Niedermeyer and Lopes da Silva, 1994).

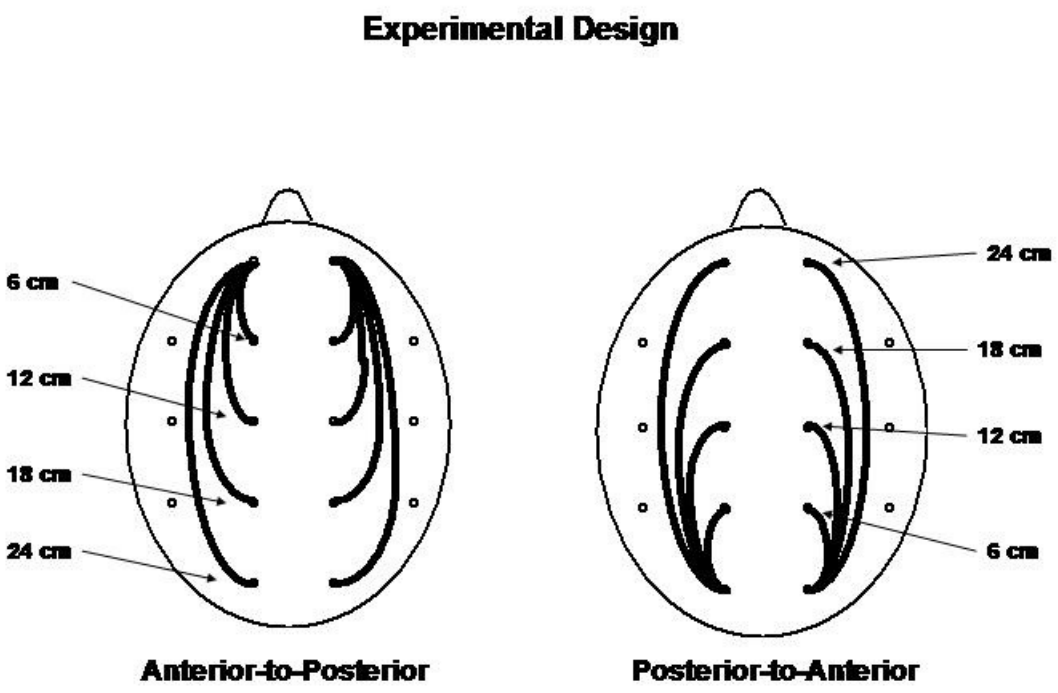

Fig. 1 – Experimental design. Left head diagram shows the location of electrodes for the computation of coherence and phase differences in the anterior-to-posterior direction. Right head diagram shows the location of electrodes in the posterior-to-anterior direction. Local distances (6 cm) are in adjacent electrode combinations (O1/2-P3/4 and Fp1/2-F3/4). Longest distance (24 cm) electrode combinations are Fp1/2-O1/2.

2.3 – Complex Demodulation and Joint-Time-Frequency-Analysis

Complex demodulation was used in a joint-time-frequency-analysis (JTFA) to compute instantaneous coherence and phase-differences (Granger and Hatanaka, 1964; Otnes and Enochson, 1978; Bloomfield, 2000). This method is an analytic linear shift-invariant transform that first multiplies a time series by the complex function of a sine and cosine at a specific center frequency (Center frequency = 10.0 Hz) followed by a low pass filter (6^{th} order low-pass Butterworth, bandwidth = 2.0 Hz) which removes all but very low frequencies (shifts frequency to 0) and transforms the time series into instantaneous amplitude and phase and an "instantaneous" spectrum (Bloomfield, 2000). We place quotations around the term "instantaneous" to emphasize that, as with the Hilbert transform, there is always a trade-off between time resolution and frequency resolution. The broader the band width the higher the

time resolution but the lower the frequency resolution and vice versa. Mathematically, complex demodulation is defined as an analytic transform (Z transform) that involves the multiplication of a discrete time series $\{x_t, t = 1, \ldots, n\}$ by sine $\omega_0 t$ and cos $\omega_0 t$ giving

$$x_t' = x_t \sin \omega_0 t \quad (1)$$

and

$$x_t'' = x_t \cos \omega_0 t \quad (2)$$

and then apply a low pass filter F to produce the instantaneous time series, Z_t' and Z_t'' where the sine and cosine time series are defined as:

$$Z_t' = F(x_t \sin \omega_0 t) \quad (3)$$

$$Z_t'' = F(x_t \cos \omega_0 t) \quad (4)$$

and

$$2\left[(Z_t')^2 + (Z_t'')^2\right]^{1/2} \quad (5)$$

is an estimate of the instantaneous amplitude of the frequency ω_0 at time t and

$$\tan^{-1} \frac{Z_t'}{Z_t''} \quad (6)$$

is an estimate of the instantaneous phase at time t. At this step the complex demodulation transform is the same as the Hilbert transform (Pikovsky et al, 2003, p. 362; Oppenheim and Schaefer, 1975).

The instantaneous cross-spectrum is computed when there are two time series $\{y_t, t = 1, .$

. . , n} and {y'$_t$, t = 1, . . . , n} and if F [ ] is a filter passing only frequencies near zero, then, as above $R_t^2 = F[y_t \sin\omega_0 t]^2 + F[y_t \cos\omega_0 t]^2 = \left|F\left[y_t e^{i\omega_0 t}\right]^2\right|$ is the estimate of the amplitude of frequency ω_0 at time t and $\varphi_t = \tan^{-1}\left(\frac{F[y_t \sin\omega_0 t]}{F[y_t \cos\omega_0 t]}\right)$ is an estimate of the phase of frequency ω_0 at time t and therefore,

$$F\left[y_t e^{i\omega_0 t}\right] = R_t e^{i\varphi_t}, \tag{7}$$

and likewise,

$$F\left[y'_t e^{i\omega_0 t}\right] = R'_t e^{i\varphi_t} \tag{8}$$

The instantaneous cross-spectrum is

$$V_t = F\left[y_t e^{i\omega_0 t}\right] F\left[y'_t e^{-i\omega_0 t}\right] = R_t R'_t e^{i[\varphi_t - \varphi'_t]} \tag{9}$$

and the instantaneous coherence is

$$\frac{|V_t|}{R_t^2 R_t'^2} \equiv 1 \tag{10}$$

The instantaneous phase-difference is $\varphi_t - \varphi'_t$. That is, the instantaneous phase difference is computed by estimating the instantaneous phase for each time series separately and then taking the difference. Instantaneous phase difference is also the arctangent of the imaginary part of V_t divided by the real part (or the instantaneous quadspectrum divided by the instantaneous cospectrum) at each time point.

2.4 – Phase Straightening

We used the phase "straightening" method of Otnes and Enochson (1978) to remove the phase angle discontinuity, i.e., where 0 and 360 are at opposite ends while in the circular

distribution $0^0 = 360^0$. The Otnes and Enochson (1978) procedure involves identifying the points in time when phase jumps from + 180^0 to – 180^0 and then adding or subtracting 360^0 depending on the direction of sign change. For example, $\Delta\theta = (180 - \varepsilon)^0 + (180 - \varepsilon)^0 = 360^0 - 2\varepsilon$ which is the same as 2ε since $-(180 - \varepsilon)^0 = 180 + \varepsilon$. This procedure results in phase being a smooth function of time and removes the discontinuities due to the arctangent function. We found that absolute phase differences without phase straightening gave similar results to the straightened phase differences. This is because the vast majority of EEG phase relationships are less than $\pm 180^0$. However, phase straightening is important when computing the first and second derivatives of the time series of phase differences because the discontinuity between – 180^0 to + 180^0 can produce artifacts. Accordingly, all of the derivatives and phase reset measures in this paper were computed after phase straightening.

2.5- Computation of the 1st and 2nd Derivatives of the Time Series of Phase Differences

The first derivative of the time series of phase-differences between all pair wise combinations of two channels was computed in order to detect advancements and reductions of phase-differences. The Savitzgy-Golay procedure was used to compute the first derivatives of the time series of instantaneous phase differences using a window length of 3 time points and the polynomial degree of 2 (Savitzgy-Golay, 1964; Press et al, 1994). The units of the 1st derivative are in degrees/point which was normalized to degrees per centisecond (i.e., degrees/cs = degrees/100 msec). The second derivative was computed using a window length of 5 time points and a polynomial degree of 3 and the units are degrees per centiseconds squared (i.e., degrees/cs^2 = degrees/100 msec.^{2}).

2.6 – Calculation of Phase Reset

The time series of 1st derivatives of the phase difference from any pair of electrodes was first rectified to the absolute value of the 1st derivative (see fig. 2). The sign or direction of a phase shift is arbitrary since two oscillating events may "spontaneously" adjust phase with no starting point (Pikovsky et al, 2003: Tass, 2007). The onset of a phase shift was defined as a significant absolute first derivative of the time series of phase differences between two channels, i.e., $d(\varphi_t - \varphi'_t)/dt > 0$, criterion bounds = 5^0. Phase stability or phase locking is defined as that period of time after a phase shift where there is a stable near zero first derivative of the instantaneous phase differences or $d(\varphi_t - \varphi'_t)/dt \approx 0$. The criteria for a significant 1st derivative is important and in the present study a threshold criteria of 5^0 was selected because it was > 3

standard deviations where the mean phase shift ranged from 25 deg/cs to 45 deg/cs. Changing the threshold to higher values was not significant, however, eliminating the threshold resulted in greater "noise" and therefore the criteria of 5^0 is an adequate criteria. As pointed out by Blackstone and Williams (2004) visual inspection of the data is the best method for selecting an arbitrary threshold value and the threshold value itself is less important than keeping the threshold constant for all subjects and all conditions. Figure two illustrates the concept of phase reset. Phase differences over time on the unit circle are measured by the length of the unit vector r. Coherence is a measure of phase consistency or phase clustering on the unit circle as measured by the length of the unit vector r. The illustration in figure 2 shows that the resultant vector $r_1 = r_2$ and therefore coherence when averaged over time ≈ 1.0 even though there is a brief phase shift. As the number of phase shifts per unit time increases then coherence declines because coherence is directly related to the average amount of phase locking or phase synchrony (Bendat and Piersol, 1980).

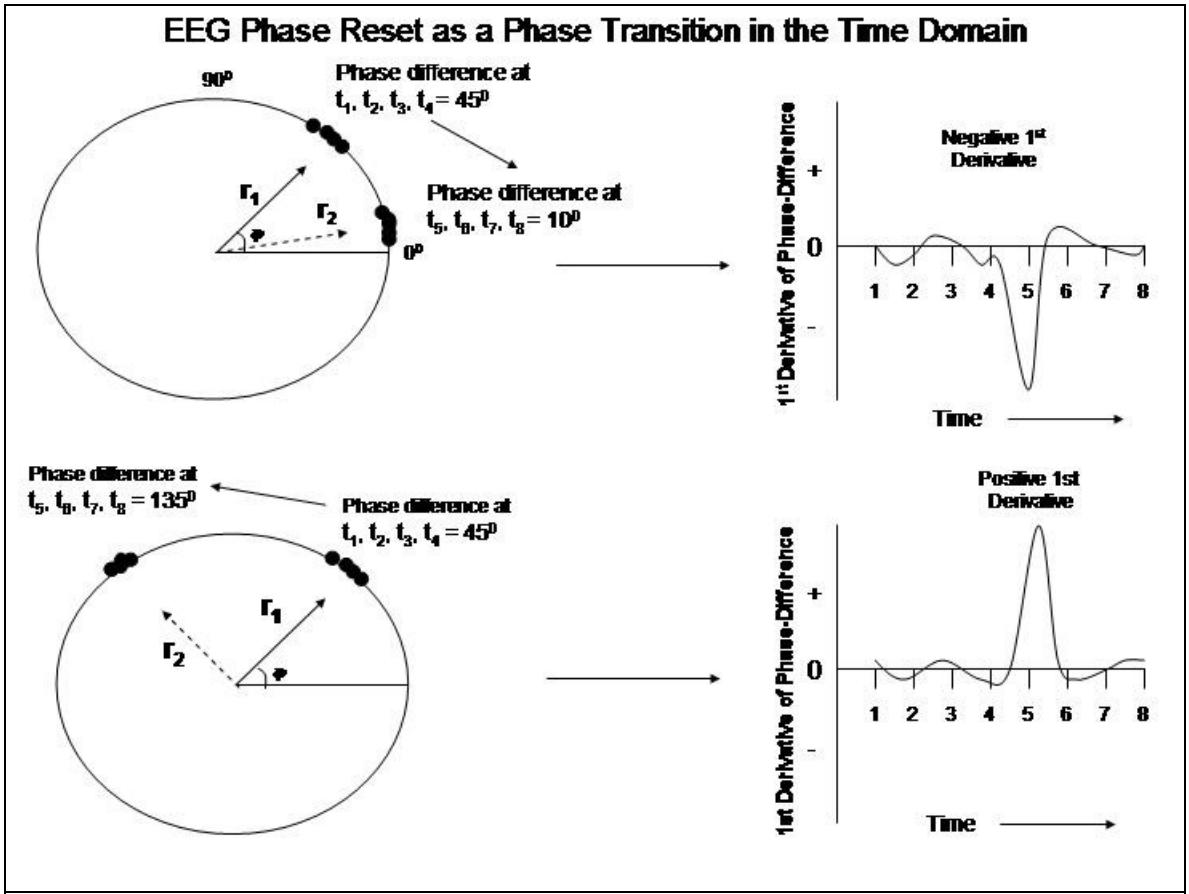

Fig. 2 – Illustrations of phase reset. Left is the unit circle in which there is a clustering of phase angles and thus high coherence as measured by the length of the unit vector r. The top row is an example of phase reduction and the top right is a time series of the

approximated 1st derivative of the instantaneous phase differences for the time series t_1, t_2, t_3, t_4 at mean phase angle = 45^0 and t_5,t_6,t_7, t_8 at mean phase angle = 10^0. The vector r1 = 45^0 occurs first in time and the vector r2 = 10^0 and 135^0 (see bottom left) occurs later in time. Phase reset is defined by a sudden change in phase difference followed by a period of phase locking. The onset of Phase Reset is between time point 4 and 5 where the 1st derivative is a maximum. The 1st derivative near zero is when there is phase locking or phase locking and little change in phase difference over time. The bottom row is an example of phase advancement and the bottom right is the 1st derivative time series. The sign or direction of phase reset in a pair of EEG electrodes is arbitrary since there is no absolute "starting point" and phase shifts are often "spontaneous" and not driven by external events, i.e., self-organizing criticality. When the absolute 1st derivative ≈ 0 then two oscillating events are in phase locking and represent a stable state independent of the direction of phase shift.

Figure 3 shows the time markers and definitions used in this study. As mentioned above the peak of the absolute 1st derivative was used in the detection of the onset and offset of a phase shift and the second derivative was used to detect the inflection point which defines the full-width-half-maximum (FWHM) and phase shift duration. As seen in Figure 3, Phase Reset (PR) is composed of two events: 1- a phase shift of a finite duration (SD) and 2, followed by an extended period of phase locking as measured by the phase locking interval (LI) and PR = SD + SI. Phase Shift duration (SD) is the interval of time from the onset of phase shift to the termination of phase shift where the termination is defined by two conditions: 1- a peak in the 1st derivative (i.e., 1st derivative changes sign from positive to zero to negative) and, 2- a peak in the 2nd derivative or inflection on the declining side of the time series of first derivatives. The peak of the 2nd derivative marked the end of the phase shift period. Phase shift duration is the difference in time between phase shift onset and phase shift offset or $SD(t) = S(t)_{onset} - S(t)_{offset}$. Phase locking interval (LI) was defined as the interval of time between the end of a significant phase shift (i.e., peak of the 2nd derivative) and the beginning of a subsequent significant phase shift, i.e., marked by the peak of the 2nd derivative and the presence of a peak in the 1st derivative or $SI(t) = S(t)_{offset} - S(t)_{onset}$ See figure 3 is a diagram of phase shift duration and phase locking intervals. In summary, two measures of phase dynamics were computed: 1- Phase shift duration (msec) (SD) and, 2- Phase locking interval (msec) (LI). Figure three illustrates the phase reset metrics and figure four shows an example of the computation of phase reset metrics in a single subject.

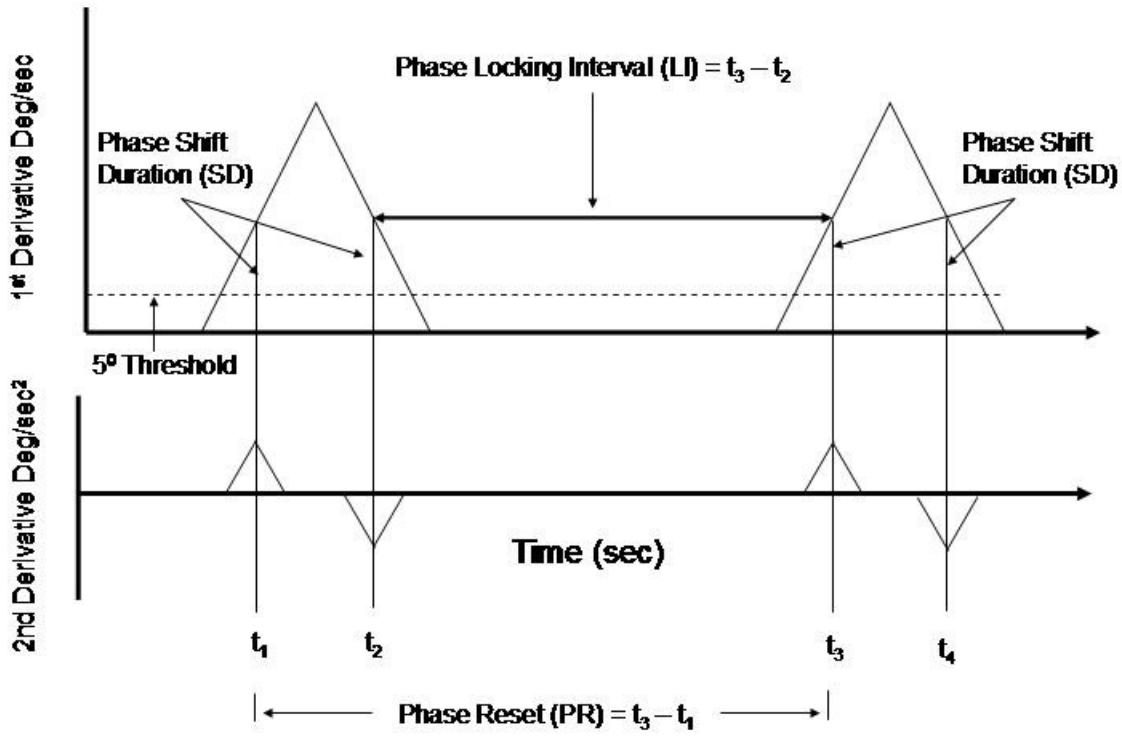

Fig. 3- Diagram of phase reset metrics. Phase shift (PS) onset was defined at the time point when a significant 1st derivative occurred ($\geq 5^0$ /centisecond) followed by a peak in the 1st derivative, phase shift duration (SD) was defined as the time from onset of the phase shift defined by the positive peak of the 2nd derivative to the offset of the phase shift defined by the negative peak of the 2nd derivative. The phase locking interval (LI) was defined as the interval of time between the onset of a phase shift and the onset of a subsequent phase shift. Phase reset interval (PRI) is composed of two events: 1- a phase shift and 2- a period of locking following the phase shift where the 1st derivative ≈ 0 or PRI = SD + LI.

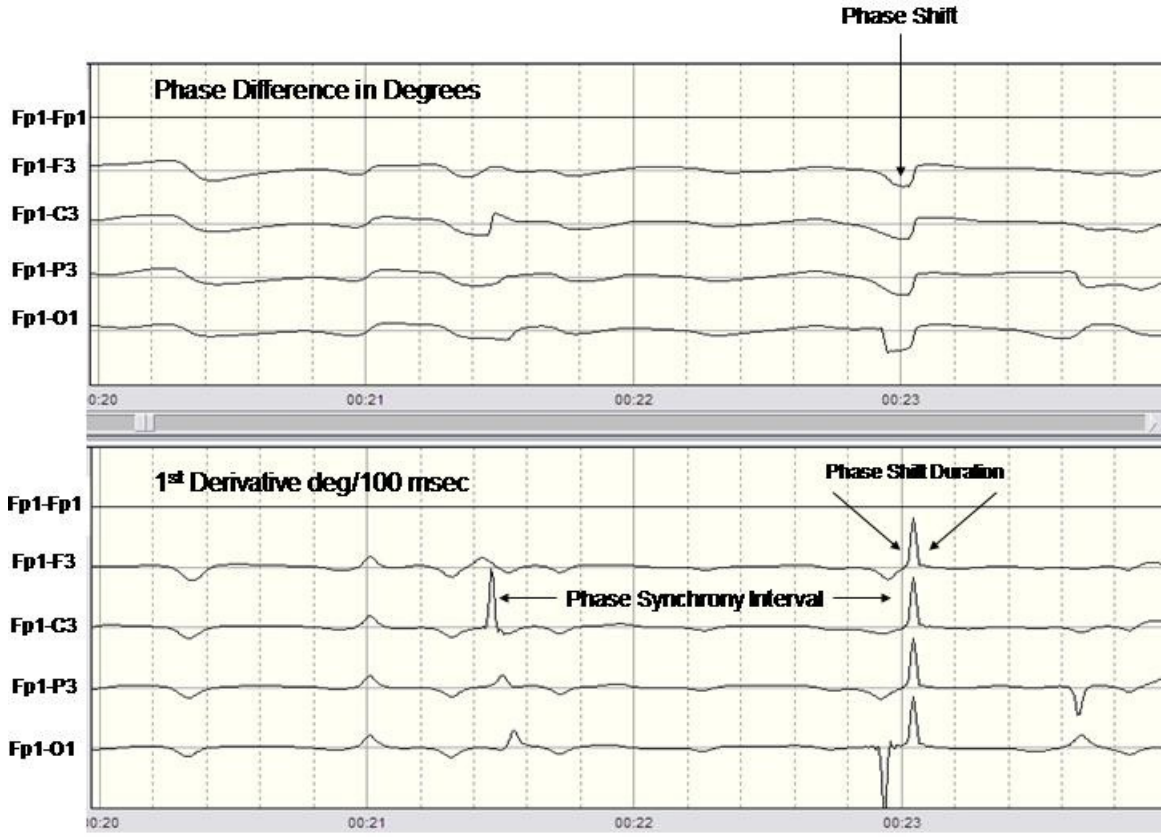

Fig. 4- Example from one subject. Top are the EEG phase differences between Fp1-F3, Fp1-C3, Fp1-P3 and Fp1-O1 in degrees. Bottom are the 1st derivatives of the phase differences in the top traces in degrees/centiseconds. A 1st derivative $\geq 5^0$ /cs marked the onset of a phase shift and an interval of time following the phase shift where the 1st derivative ≈ 0 defined the phase locking interval as described in figure 3.

2.7 – Sliding Averages

In order to increase temporal resolution one year sliding averages of EEG phase differences were computed. The procedure involved computing means and standard deviations for phase locking intervals and phase shift intervals over a one year period, e.g., birth to 1 year, then computing means and standard deviations from 0.25 years to 1.25 years, then a mean and standard deviation for the ages from 0.5 years to 1.5 years, etc. This resulted in a 75% overlap of subjects per mean with totally unique subjects on a one year interval. The sliding average procedure produced 64 equally spaced mean values with a 0.25 year resolution. Table I shows the age range per bin, the mean ages per bin and the number of subjects per age group from mean age of 0.4 years to 16.2 years. Relative small Ns were present from 0.4 to 1.4 years of age and larger sample sizes (max N = 50) were present beyond one year of age. In spite of the relatively

small sample sizes at 0.4 years to 1.4 years the mean values of phase shift and phase reset were well behaved (see figs. 7 & 8). The overall average number of subjects per age bin = 28.5.

Table I

AGE BINs	MEAN AGE	N-SIZE	AGE BINs	MEAN AGE	N-SIZE
0.00-1.00	0.4	7	8.00-9.00	8.4	32
0.25-1.25	0.7	5	8.25-9.25	8.7	28
0.50-1.50	1.1	7	8.50-9.50	9.0	26
0.75-1.75	1.4	9	8.75-9.75	9.3	29
1.00-2.00	1.6	11	9.00-10.00	9.6	38
1.25-2.25	1.8	14	9.25-10.25	9.8	45
1.50-2.50	2.0	14	9.50-10.50	10.0	46
1.75-2.75	2.2	11	9.75-10.75	10.2	45
2.00-3.00	2.6	14	10.00-11.00	10.4	40
2.25-3.25	2.8	13	10.25-11.25	10.8	40
2.50-3.50	3.0	13	10.50-11.50	11.0	43
2.75-3.75	3.2	14	10.75-11.75	11.3	47
3.00-4.00	3.5	13	11.00-12.00	11.5	50
3.25-4.25	3.9	15	11.25-12.25	11.7	42
3.50-4.50	4.0	15	11.50-12.50	11.9	40
3.75-4.75	4.2	17	11.75-12.75	12.3	39
4.00-5.00	4.4	16	12.00-13.00	12.5	39
4.25-5.25	4.9	19	12.25-13.25	12.7	41
4.50-5.50	5.0	23	12.50-13.50	13.0	41
4.75-5.75	5.3	28	12.75-13.75	13.3	38
5.00-6.00	5.5	34	13.00-14.00	13.5	41
5.25-6.25	5.8	36	13.25-14.25	13.7	38
5.50-6.50	6.0	35	13.50-14.50	13.9	36
5.75-6.75	6.2	34	13.75-14.75	14.2	30
6.00-7.00	6.5	38	14.00-15.00	14.4	24
6.25-7.25	6.8	33	14.25-15.25	14.7	23
6.50-7.50	7.0	40	14.50-15.50	14.9	20
6.75-7.75	7.3	44	14.75-15.75	15.3	17
7.00-8.00	7.5	47	15.00-16.00	15.5	16
7.25-8.25	7.7	48	15.25-16.25	15.7	12
7.50-8.50	8.0	45	15.50-16.50	15.8	11
7.75-8.75	8.2	40	15.75-16.75	16.2	12

Table I – Age ranges, mean ages and the number of subjects per age bin using sliding average computation.

2.8 – Spectral Analyses of 1/f distribution

To evaluate possible 1/f spectral distributions the fast Fourier transform (FFT) of the time series of the 1st derivative of phase differences were computed for individual subjects using

edited EEG data. The FFT epoch length was 2 seconds and the sample rate was 128 Hz. Computations were first conducted on the entire edited EEG record (58 sec to 2 min 17 sec) and then separate selections of periods of phase shift and phase locking were subjected to separate FFT analyses in order to determine if the spectra were different between the phase locking vs. the phase shift periods in the EEG record. Tests of the 1/f distribution involved plotting the $\log_{10}$ transforms of frequency and magnitude and then a linear regression was used to determine the slope (α coefficient) and intercept of the linear fit.

2.9 – Spectral Analyses of Developmental Ultraslow Oscillations During the Lifespan

As explained previously, the sliding averages produced 64 equally spaced mean values of phase shift duration and phase locking intervals in each electrode pairing (at 3 month or 0.25 year resolution) from 0.4 years to 16.2 years. This resulted in a developmental time series of equally spaced mean ages for phase shift duration and phase locking intervals which were then spectrally analyzed. The Fast Fourier Transform (FFT) was used to analyze the frequency spectrum of the developmental trajectories of phase shift and phase locking. Detrending was used prior to the FFT to remove the low frequency developmental trends in order to analyze the frequency and power of rhythmic changes during the developmental period. The number of time points = 64, and the epoch length or Lifespan = 16.2 years. This produced a frequency resolution of 6 months and a maximum frequency of 32 cycles per epoch. The units of frequency were cycles per lifespan (cpl) and wavelength (λ) = 16.2/cpl. The units of frequency are cpl. The magnitude of the spectrum plotted on the y-axis are milliseconds/cycle/lifespan or msec/cpl.

3.0 – Results

3.1 – 1/f Phase Reset Distributions

As discussed in the introduction, the human EEG is often characterized by 1/f distributions which are revealed by log-log plots of the power spectrum (Freeman et al, 2003; 2006; Buzaki, 2006). All of the subjects exhibited 1/f distributions of the 1st derivative of phase differences. Figure 5 shows examples of linear regression fits of the log-log plots of the

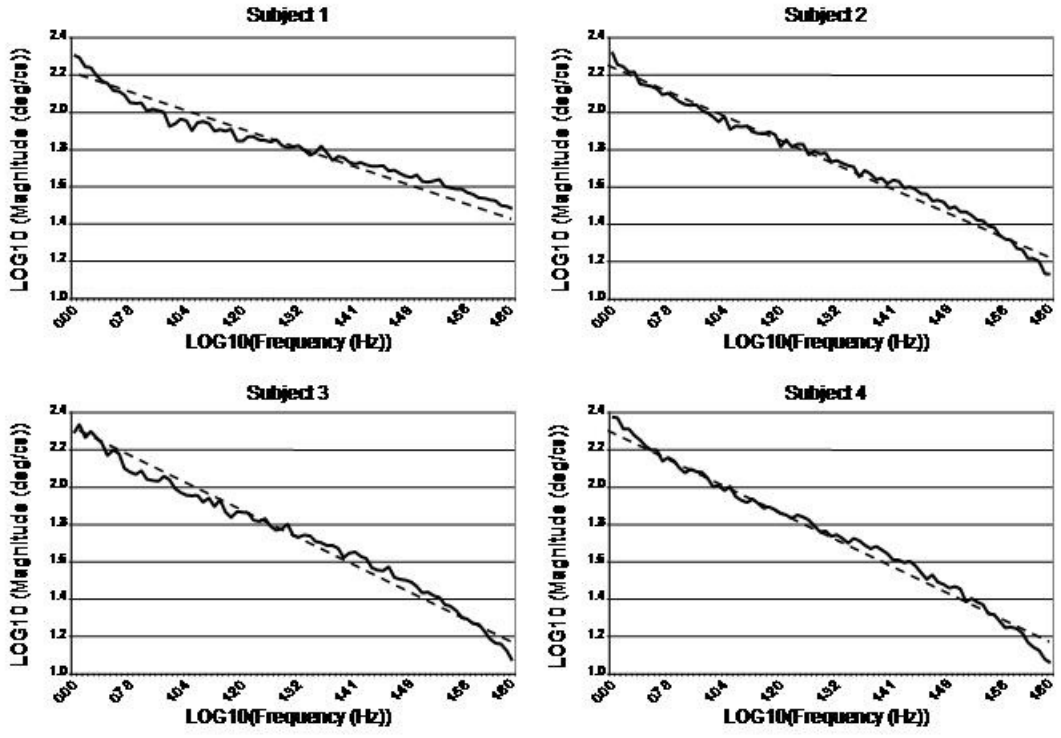

Fig. 5- Examples of the log-log plots of the FFT of the 1st derivatives of EEG phase differences in the anterior-to-posterior direction. Solid line is the FFT spectral values and the dotted line is the linear regression fits to the spectral values. Table I shows the slope or α exponents in the $1/f^{\alpha}$ equation.

power spectrum of the 1st derivative of phase differences in four subjects in the anterior-to-posterior direction. Very similar spectra were obtained independent of direction of hemisphere. Table II shows the slope or α values, the intercept and the regression correlation coefficients which all yielded $1/f^{\alpha}$ spectral distributions with a range from – 0.86 to – 0.54 and the average α = -0.76. To further investigate the nature of the 1/f distribution, sub-component analyses were conducted by selecting the 1st derivative of phase difference during phase reset by separately selecting the phase shift periods and phase locking periods and then spectrally analyzing the two different data selections. Frequency and magnitude were $\log_{10}$ transformed and linear regression fits were conducted in order to determine the slopes of the spectra. The results of the sub-component analyses are shown in figure 6 and Table III. In all instances and in all subjects

Table II
Linear Regression Fit to the Log-Log Plot of the Power Spectrum of EEG Phase Reset

REGRESSIONs	Subject 1	Subject 2	Subject 3	Subject 4
SLOPE – α	0.5419	0.7543	0.8066	0.8634
CORRELATION	0.966	0.917	0.914	0.918
SIGNIFICANT	P<.0001	P<.0001	P<.0001	P<.0001

Table II – The results of the linear regression fit to the log-log plot of the power spectra in Figure 6. The sign of the correlation and α is in accordance with $1/f^{\alpha}$.

the slope of the linear fit was > 1.0 for phase locking and < 1.0 for phase shift periods. The average slope or α coefficient was close to 1.0 with a mean = 1.0466. As seen in Table III, there were statistically significant differences in slope (i.e., α) between periods of phase shift vs. periods of phase locking where the slope was always steeper for phase locking than phase shift. Although all of the regression fits were statistically significant, nonetheless, the linear fit for phase locking accounted for less variance than for phase shift duration which is likely due to the exponential shape of the phase locking spectral distribution.

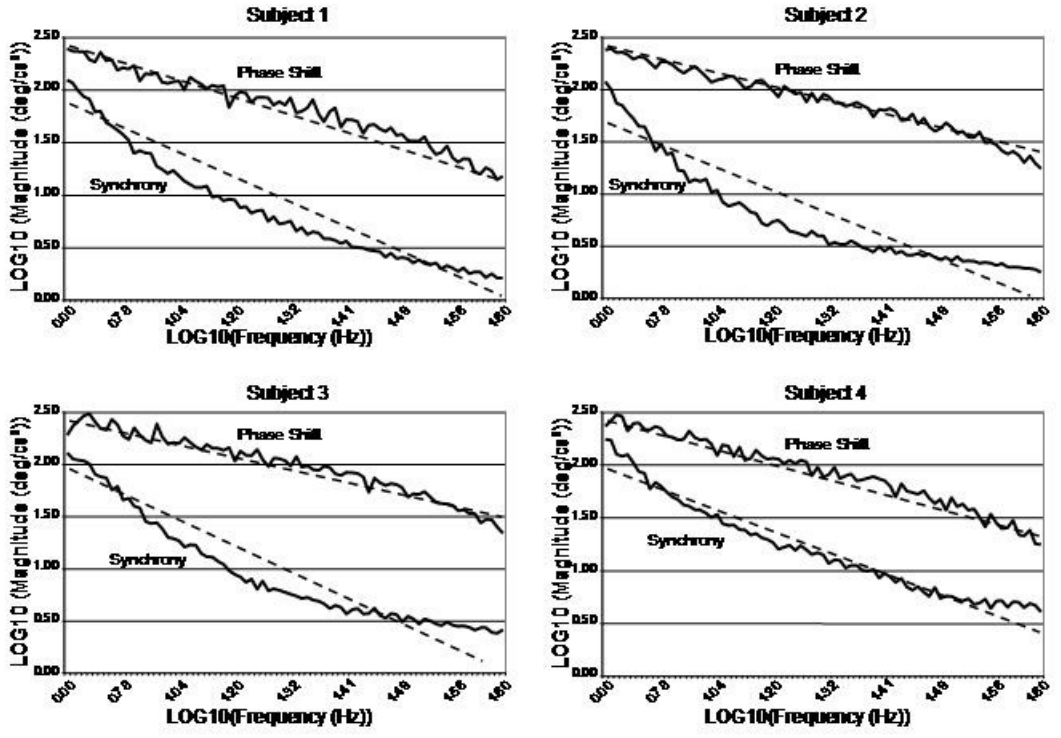

Fig. 6- Log-log plots of the Fourier analyses of the 1st derivative of phase differences during periods of phase locking versus periods of phase shift in the four different subjects in figure 6. Solid line is the FFT spectral values and the dotted line is the linear regression fits to the spectral values. A $1/f^{\alpha}$ distribution is present in all instances in which the slope coefficients were higher for the phase locking periods in comparison to the phase shift periods. Table II shows the differences in slopes and the1/f alpha coefficients for phase shifting vs. phase locking as well as the average $\alpha \approx 1$.

Table III shows the alpha slope values and age regression correlations and t-tests between the spectral distributions for phase shift vs. phase locking intervals for the four sample subjects in figure 6. The α values for phase shift were statistically significantly smaller than the α values for phase locking and the average α value was close to 1.0 which indicates that decomposition of the log-log spectral distribution into sub-components of phase shift vs. phase locking is useful in order to reveal more of the underlying EEG dynamics.

Table III
Linear Regression Fit of Separate Log-Log Spectral Analyses
of Phase Shift and Phase Locking

REGRESSIONs	Subject 1	Subject 2	Subject 3	Subject 4
Phase Lock - α	1.4223	1.3207	1.3764	1.2088
Phase Shift - α	0.8226	0.7453	0.6826	0.7938
Average - α	1.1225	1.0330	1.0295	1.0013
T-Test	p < .0001	p < .0001	p < .0001	p < .0001

Table III- Summary of the log-log regression fits and estimates of the slope (i.e., alpha) for the same subjects as in figs. 6 & 7. The alpha values in the $1/f^{\alpha}$ distributions are shown for the phase locking vs. phase shift periods. The average α values were near to 1.0. The sub-component analyses of phase shift vs. phase locking reveals interesting differences in the slope or alpha of the 1/f distribution for phase shift vs. phase locking.

3.2 – Development of Phase Shift Duration

Figure 7 shows the mean duration of phase shift in the alpha frequency band from 0.4 to 16.2 years of age. The top row are mean phase shift duration values in the anterior-to-posterior direction (see fig. 1) and the bottom row are the posterior-to-anterior electrode combinations. The left column are the mean phase reset durations for the left hemisphere and

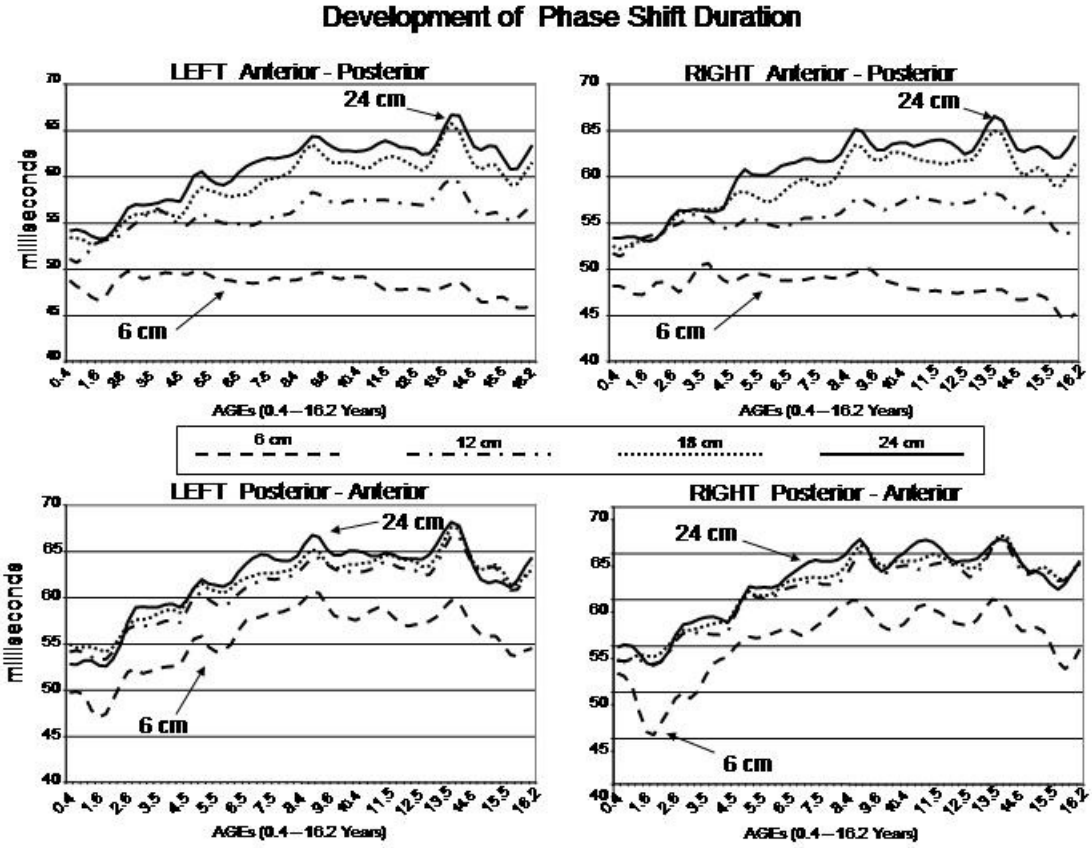

Fig. 7- Mean EEG phase shift duration from 0.44 years of age to 16.22 years of age. Top row are from the anterior-to-posterior electrode combinations and bottom row are from the posterior-to-anterior electrode combinations (see Fig. 1). The left column is from the left hemisphere and the right column is from the right hemisphere. It can be seen that phase shift duration increases in most electrode combinations but decreases in the short inter-electrode distance (6 cm) in the anterior-to-posterior direction.

the right column are the right hemisphere values. It can be seen that there were oscillations and sudden changes in the mean duration of phase shift and there was a steady increase in the mean duration of phase shift as a function of age in the long inter-electrode distances (18 cm & 24 cm) and reduced phase shift duration in the short inter-electrode distance (6 cm) in anterior-posterior directions. In the posterior-anterior direction, an increase in phase shift duration was present as a function of age in all inter-electrode distances, although the long inter-electrode distances (18 cm & 24 cm) exhibited a more pronounced increase in phase duration with age than the short inter-electrode distances (6 cm).

Table IV shows the results of a linear fit of the mean duration of phase shift as a function of age for all electrode pairings. It can be seen in Table IV that there were statistically significant negative

slopes in the short inter-electrode distance (6 cm) in the anterior-posterior direction and positive slopes in all other instances. Statistically significant age regressions were present for all of the developmental trajectories.

Table IV
Age Regression of Phase Shift Duration

LEFT Anterior - Posterior

	6cm	12cm	18cm	24cm
SLOPE	-0.0001	0.0003	0.0006	0.0006
INTERCEPT	0.0494	0.0536	0.0544	0.0554
CORRELATION	-0.534	0.700	0.833	0.844
SIGNIFICANT	P<.0001	P<.0001	P<.0001	P<.0001

RIGHT Anterior - Posterior

	6cm	12cm	18cm	24cm
SLOPE	-0.0002	0.0002	0.0006	0.0007
INTERCEPT	0.0494	0.0538	0.0543	0.0548
CORRELATION	-0.577	0.633	0.823	0.861
SIGNIFICANT	P<.0001	P<.0001	P<.0001	P<.0001

LEFT Posterior - Anterior

	6cm	12cm	18cm	24cm
SLOPE	0.0005	0.0006	0.0006	0.0006
INTERCEPT	0.0516	0.0565	0.0564	0.0554
CORRELATION	0.634	0.731	0.819	0.844
SIGNIFICANT	P<.0001	P<.0001	P<.0001	P<.0001

RIGHT Posterior - Anterior

	6cm	12cm	18cm	24cm
SLOPE	0.0005	0.0007	0.0007	0.0007
INTERCEPT	0.0511	0.0563	0.0555	0.0548
CORRELATION	0.628	0.771	0.841	0.861
SIGNIFICANT	P<.0001	P<.0001	P<.0001	P<.0001

Table IV – Linear regression statistics for mean phase shift duration from 0.44 years to 16.22 years of age. The top two rows are from the anterior-to-posterior direction and the bottom two rows are from the posterior-to-anterior direction. Short Inter-electrode distance (6 cm) in the anterior-to-posterior direction exhibited a negative slope as a function of age while all other inter-electrode distances and direction exhibited positive slopes as a function of age. The y-intercept, regression correlation and statistical significance are also shown.

Multivariate analyses of variance (MANOVA) were conducted with the factors being direction (anterior-to-posterior vs. posterior-to-anterior), left hemisphere vs. right hemisphere and distance (6 cm, 12 cm, 18 cm & 24 cm). No significant left vs. right hemisphere affect was present ($F= 0.2345$, $P < 0.628$). However, there was a statistically significant direction affect ($F = 303.73$, $P < .0001$) with a statistically significant Bonferroni post hoc test ($P < .0001$). There was also a statically significant distance affect ($F = 350.21$, $P < .0001$) with statistically significant Bonferroni post hoc tests ($P > ,0001$) for all inter-electrode distances except for 24 cm – 18 cm ($P < 0.68$).

3.3 – Development of the Phase Locking Interval

Figure 8 shows the mean phase locking interval in the alpha frequency band from 0.4 to 16.2 years of age. The top row are mean phase locking interval values in the anterior-to-posterior direction (see fig. 1) and the bottom row are the posterior-to-anterior electrode combinations. The left column are the mean phase locking intervals for the left hemisphere and

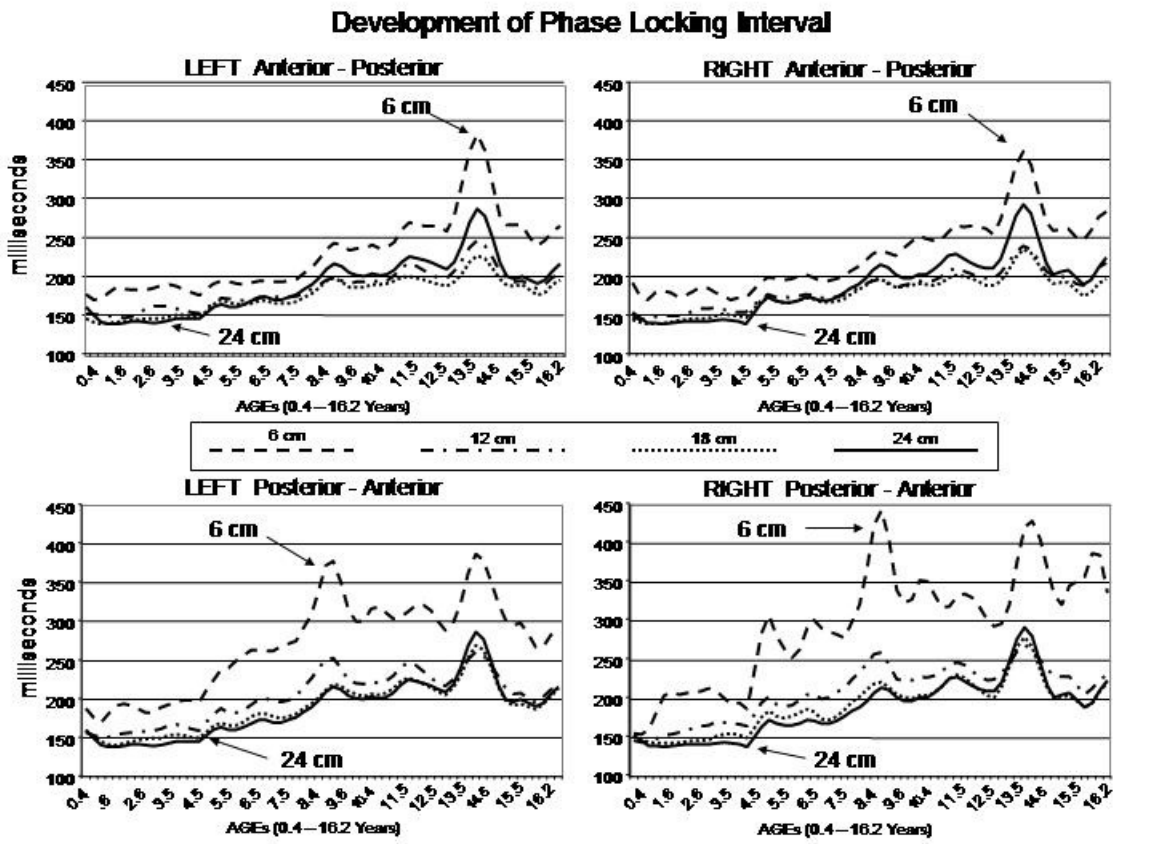

Fig. 8- Mean EEG phase locking intervals from 0.44 years of age to 16.22 years of age. Top row are from the anterior-to-posterior electrode combinations and bottom row are from the posterior-to-anterior electrode combinations (see Fig. 1). The left column is from the left hemisphere and the right column is from the right hemisphere. Growth spurts and oscillations during development are seen. Also, it can be seen that phase locking intervals increase as a function of age in all electrode combinations.

the right column are the right hemisphere values. It can be seen that there were oscillations and sudden changes in the mean phase locking intervals and there was a steady increase in the mean phase locking interval as a function of age in the short inter-electrode distance (6 cm) with less increased phase locking intervals in the long inter-electrode distances. Sudden increases in the mean phase locking interval were present n all electrode combinations at ages 9 and 14 years, especially in the short inter-electrode distances (6 cm) and in the posterior-to-anterior direction.

Table V shows the results of a linear fit of the mean phase locking interval as a function of age for all electrode pairings. It can be seen in Table V that there were statistically significant positive slopes in all instances. The short inter-electrode distance (6 cm) exhibited a steeper developmental slope in the posterior-to-anterior direction than in the anterior-to-posterior direction.

Table V

Age Regression of Phase Locking Interval

LEFT Anterior - Posterior

	6cm	12cm	18cm	24cm
SLOPE	0.0087	0.0045	0.0043	0.0065
INTERCEPT	0.1550	0.1457	0.1392	0.1324
CORRELATION	0.825	0.852	0.868	0.831
SIGNIFICANT	P<.0001	P<.0001	P<.0001	P<.0001

RIGHT Anterior - Posterior

	6cm	12cm	18cm	24cm
SLOPE	0.0087	0.0047	0.0044	0.0068
INTERCEPT	0.1538	0.1440	0.1395	0.1308
CORRELATION	0.870	0.905	0.859	0.840
SIGNIFICANT	P<.0001	P<.0001	P<.0001	P<.0001

LEFT Posterior - Anterior

	6cm	12cm	18cm	24cm
SLOPE	0.0101	0.0055	0.0056	0.0065
INTERCEPT	0.1871	0.1568	0.1419	0.1324
CORRELATION	0.783	0.781	0.819	0.831
SIGNIFICANT	P<.0001	P<.0001	P<.0001	P<.0001

RIGHT Posterior - Anterior

	6cm	12cm	18cm	24cm
SLOPE	0.0131	0.0063	0.0059	0.0068
INTERCEPT	0.1867	0.1566	0.1423	0.1308
CORRELATION	0.824	0.833	0.821	0.840
SIGNIFICANT	P<.0001	P<.0001	P<.0001	P<.0001

Table V – Linear regression statistics for mean phase locking intervals from 0.44 years to 16.22 years of age. The top two rows are from the anterior-to-posterior direction and the bottom two rows are from the Posterior-to-anterior direction. The y-intercept, regression correlation and statistical significance are also shown.

Multivariate analyses of variance (MANOVA) were conducted with the factors being

direction (anterior-to-posterior vs. posterior-to-anterior), left hemisphere vs. right hemisphere and distance (6 cm, 12 cm, 18 cm & 24 cm). No significant left vs. right hemisphere affect was present (F= 3.033, P < 0.082). However, there was a statistically significant direction affect (F = 82.02, P < .0001) with a statistically significant Bonferroni post hoc test (P < .0001). There was also a statically significant distance affect (F = 173.55, P < .0001) with statistically significant Bonferroni post hoc tests (P > ,0001) for all inter-electrode distances except for 24 cm – 12 cm (P < 0.271) and 24 cm – 18 cm (P < 0.783).

3.4- Relations Between EEG Phase Reset and Coherence

Coherence is a measure of phase stability and one would expect a positive correlation between the duration of phase locking and coherence. We tested this hypothesis using a Pearson product correlation coefficient of the developmental time series of coherence and phase shift duration and phase locking interval in the short inter-electrode distances (6 cm). Table VI shows the average correlation of the short inter-electrode distance measures in which there was a negative correlation between coherence and phase shift duration (i.e., inverse relationship to "unstable phase dynamics") and a positive correlation between coherence and phase locking intervals (i.e., direct relationship to "Stability"). The hypothesis of a positive relationship between coherence and phase locking was confirmed. As expected there was an inverse relationship between phase shift duration ("unstable phase dynamics") and the phase locking interval ("stability"), however, the correlations were relatively small indicating that the majority of variance is unaccounted for when correlating phase shift durations with phase locking intervals.

Table VI
Correlations between Coherence and Phase Shift Duration
and Phase Locking Interval

	Phase Shift	Phase Locking
Coherence	- 0.547	0.863
Phase Shift	---------	- 0.386
Phase Locking	- 0.386	--------

Table VI- Average correlations between coherence and phase shift duration ("Unstable phase dynamics") and phase locking ("Stability") at the short inter-electrode distance (6 cm). There was a negative correlation between coherence and "Unstable phase dynamics" and a positive correlation between coherence and "stability".

To further explore the nature of phase shift and phase duration the temporal boundaries and frequency distributions were studied. Figure 9 shows the frequency distribution of phase shift durations (Top) and the phase locking intervals (Bottom) for short and long distance connections (average of left and right hemisphere) in 215 subjects between 10 and 16.67 years of age. Phase shift duration exhibited temporal boundaries or “window lengths” with no durations

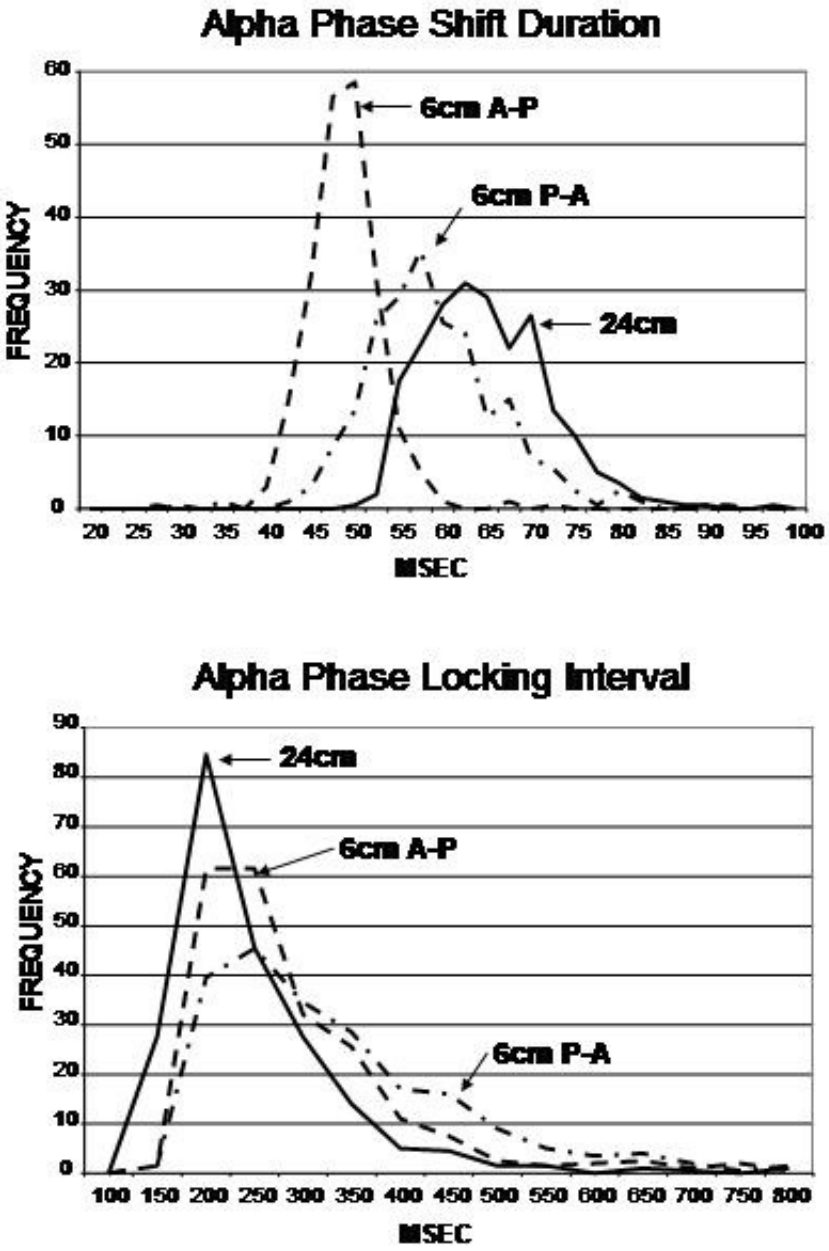

Fig. 9 – Frequency histograms of phase shift duration (Top) and phase locking intervals (Bottom) from 215 subjects between 10 and 16.67 years of age. 5 cm anterior-to-posterior (AP) inter-electrode distance, 6 cm inter-electrode distance for posterior-to-anterior direction (PA) and the long (24 cm) inter-electrode distance which is the same for AP and PA (see fig. 1). Left and right hemispheres were averaged together. The y-axis is the number of subjects and the x-axis is msec.

less than 25 msec and no durations greater than 100 msec. Local (6 cm) frontal distances exhibited the most peaked distribution at 45 msec duration and the long distance (24 cm) connections were shifted in peak duration by approx. 15 – 20 msec. The phase locking interval exhibited temporal boundaries or window lengths with no durations less than 150 msec and 99% of the durations less than 900 msec. The frequency distributions as a function of distance were similar although the long distance (24 cm) connections were most peaked at 200 msec and exhibited an approximate 50 msec. shift in peak duration in comparison to the local connections. Phase locking (stable dynamic) was on the average shorter and phase shift duration (unstable dynamic) was longer in the long distant connection system.

3.5 – Developmental Oscillations

Examination of figures 7 and 8 shows ultra-slow oscillations with inter-peak intervals of approximately 2 to 3 years. Spectral analyses of the developmental time series of mean phase shift duration from 0.4 years to 16.2 years for the 6 cm and 24 cm inter-electrode distances are shown in figure 10. The top row are the frontal-to-posterior electrode combinations and the bottom row are the occipital-to-anterior combinations. The left column are the left hemisphere mean FFT values and the right column are the right hemisphere values (see Fig. 1). In general there was greater developmental spectral energy in the short inter-electrode distance (6 cm) in comparison to the long inter-electrode distance (24 cm). Most of the developmental spectral energy was in the ultraslow frequency range of 1 cycle per lifespan (i.e., a wavelength of 16 years) to approximately 12 cycles per lifespan (i.e., a wavelength of 1.3 years). The highest peak frequency was 31 cycles per lifespan (i.e., a wavelength of 0.5 years or 6 months).

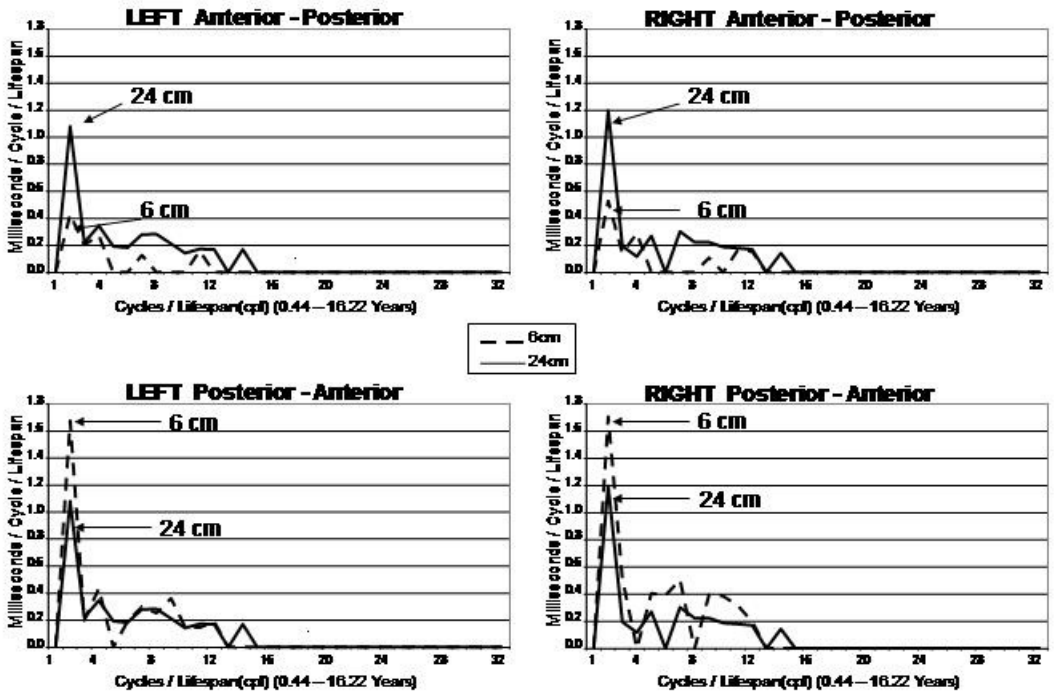

Fig. 10 – Fourier spectral analyses of the developmental trajectories of phase shift duration from 0.44 years to 16.22 years of age in short (6 cm) (dashed line) and long (24 cm) (solid line) inter-electrode distances in the anterior-to-posterior and posterior-to-anterior directions. Magnitude is on the y-axis and frequency on the x-axis. Distant inter-electrodes exhibited greater power in the anterior-to-posterior direction while local connections exhibited the greater power in the posterior-to-anterior direction.

Spectral analyses of the developmental time series of mean phase locking intervals from 0.4 years to 16.2 years for the 6 cm and 24 cm inter-electrode distances are shown in figure 11 The top row of figure 11are the anterior-to-posterior electrode combinations and the bottom row are the posterior-to-anterior combinations. The left column are the left hemisphere FFT values and the right column are the right hemisphere values (see Fig. 1). Similar to phase shift duration, phase locking exhibited most of the spectral energy in the ultraslow frequency range of 1 cycle per lifespan (i.e., a wavelength of 16 years) to approximately 20 cycles per lifespan (i.e., a wavelength of 0.8 years). Similar to phase shift duration, phase locking in the short inter-electrode distance (6 cm) was greater than the long distance (24 cm) in the posterior-to-anterior direction.

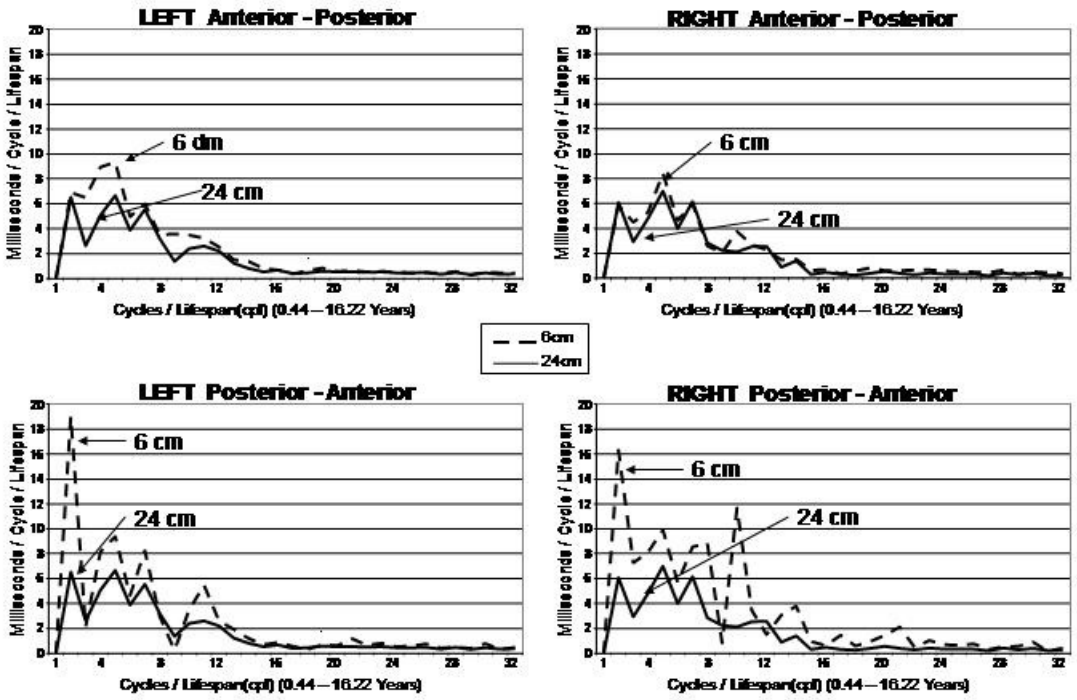

Fig. 11 – Fourier spectral analyses of the development of phase locking from 0.44 years to 16.22 years of age in short (6 cm) (dashed line) and long (24 cm) (solid line) inter-electrode distances in the anterior-to-posterior and posterior-to-anterior directions. Magnitude is on the y-axis and frequency on the x-axis. The greatest spectral energy was in the short distance inter-electrodes (6 cm) in the posterior-to-anterior direction and repetitive 8 year and 4 year and 2 year cycles. See Table VI for the lamda values in years.

Tables VII and VIII are summaries of the cycles per lifespan (cpl) and the wavelength (16 yrs/cpl) of the spectral peaks in the FFT analyses of the mean duration of phase shift and mean phase locking developmental trajectories from 0.4 years to 16.2 years shown in figures 9 & 10 respectively. Table VII shows the FFT peak values for phase shift duration over the lifespan in the frontal-to-posterior direction (Top) and for the posterior-to-anterior direction (Bottom). It can be seen that short (6 cm) and distant (24 cm) exhibited different spectra for phase shift duration and different spectra as a function of direction. In general there are more spectral peaks and greater power in the long distant inter-electrode connections (24 cm) in the anterior-to-posterior direction while there are more spectral peaks in the 6 cm distance in the posterior-to-anterior direction.

Table VI
Summary of Spectral Peaks of Phase Shift Duration

Anterior - Posterior

LEFT			
	6cm		24cm
CPL	λ (yrs)	CPL	λ (yrs)
2	8	2	8
4	4	4	4
7	2.29	7	2.29
11	1.45	8	2
		12	1.33
		14	1.14

RIGHT			
	6cm		24cm
CPL	λ	CPL	λ (yrs)
2	8	2	8
4	4	5	3.2
9	1.78	7	2.29
11	1.45	12	1.33
		14	1.14

Posterior - Anterior

LEFT			
	6cm		24cm
CPL	λ (yrs)	CPL	λ (yrs)
2	8	2	8
4	4	4	4
7	2.29	7	2.29
9	1.78	14	1.14
12	1.33		

RIGHT			
	6cm		24cm
CPL	λ (yrs)	CPL	λ (yrs)
2	8	2	8
5	3.2	5	3.2
7	2.29	7	2.29
9	1.78	14	1.14
10	1.6		

Table VI– Summary of spectral peaks of the phase shift duration in the anterior-to-posterior direction (top) and the posterior-to-anterior direction (bottom) for 6 cm and 24 cm inter-electrode distances. Lifespan = 16 years and cpl = cycles per lifespan and λ = wavelength in years or lifespan/cpl.

Table VIII are summaries of the cycles per lifespan (cpl) and the wavelength (16 yrs/cpl) for the mean phase locking developmental trajectories from 0.4 years to 16.2 years. The largest number of spectral peaks was in the posterior-to-anterior direction in the short inter-electrode distance (6 cm).

Table VII

Summary of Spectral Peaks of Phase Synchrony Interval

Anterior - Posterior

LEFT			
	6cm		24cm
CPL	λ (yrs)	CPL	λ (yrs)
2	8	2	8
4	4	5	3.2
5	3.2	7	2.29
7	2.29	11	1.45

RIGHT			
	6cm		24cm
CPL	λ (yrs)	CPL	λ (yrs)
2	8	2	8
5	3.2	5	3.2
7	2.29	7	2.29
10	1.6	12	1.33

Posterior - Anterior

LEFT			
	6cm		24cm
CPL	λ (yrs)	CPL	λ (yrs)
2	8	2	8
5	3.2	5	3.2
7	2.29	7	2.29
11	1.45		
21	0.76		

RIGHT			
	6cm		24cm
CPL	λ (yrs)	CPL	λ (yrs)
2	8	2	8
5	3.2	5	3.2
8	2	7	2.29
10	1.6	12	1.33
14	1.14	14	1.14
21	0.76		

Table VII – Summary of spectral peaks of phase locking intervals in the anterior-to-posterior direction (top) and the posterior-to-anterior direction (bottom) for 6 cm and 24 cm inter-electrode distances. Lifespan = 16 years and cpl = cycles per lifespan, and λ = wavelength in years or lifespan/cpl.

4.0 – Discussion

This study extends the investigation of the spatial and temporal properties of EEG phase reset to a large population of subjects from infancy to adolescence and focuses on brain development of phase reset in the alpha frequency band. An important finding is that the average phase shift duration (unstable dynamics) and the average phase locking interval (stability) were significantly correlated with age and exhibited different maturational trajectories, oscillations and growth spurts in the anterior-to-posterior vs. posterior-to-anterior directions (see figs. 7 & 8). A second significant finding was that the frontal phase shift duration (unstable dynamics) increased as a function of age in distant connections in contrast to posterior local connections (see fig. 7 & Table IV). The third significant finding was that phase stability increased as a function of age in both local and distant connections (see fig. 8 and Table V). A fourth significant finding was the presence of $1/f^{\alpha}$ log-log distributions near to 1 thus showing scale invariant fluctuations linked to the development of minimally stable states such as human EEG

phase reset (see figs. 5 & 6 and Tables II & III). All five null hypotheses listed in the introduction were rejected by the findings in this study.

4.2 – EEG Phase Transitions and Self-Organized Criticality

The results are consistent with self-organized criticality (SOC) models of cortical function (Bak et al, 1988; Freeman et al, 2003; 2006; Linkenkaer-Hansen et al, 2001; Le van Quyen, 2003; Stam and de Bruin, 2004; Buzsaki, 2006). Self-organized criticality was defined by Bak et al (1987;1988) as the combination of "self-organization" and "criticality" necessary to describe complex systems in which phase transitions spontaneously occur without external "tuning" or external influences. Phase reset includes "self-organization" in the form of phase locking and "criticality" in the form of rapid phase shifts. There are no known sources of the phase shift transitions themselves and thus, phase shifts are likely a widely distributed "emergent" process that spontaneously occurs in complex systems. A fundamental property of SOC is the presence of $1/f^{\alpha}$ distributions that characterize invariant scaling properties, fractal spatial statistics and long-range spatial and temporal correlations, where f = frequency and $\alpha \approx 1$ (Bak et al, 1987; 1988; Nikulin and Brismar, 2004, 2005; Parish et al, 2004). Studies by Rios and Zhang (1999) have shown that the universal properties of the $1/f^{\alpha}$ distribution are an activation-deactivation sequence of a "slow" energy addition and a "fast" energy dissipation with the additional condition of a preferred propagation direction and a limited range of energy dissipation. According to Bak et al (1987; 1988), Bak (1996) and Rios and Zang (1999) if these universality properties exist, then a 1/f distribution will be produced. EEG phase reset meets the slow and fast component criteria with rapid phase shift onsets as a "fast process" (5 msec – 20 msec) and phase locking as a comparative "slow process" (150 msec to 1 second; Freeman et al, 2006). All self-sustained oscillators, such as neurons, are characterized by the fact that they dissipate energy (Pikovsky et al, 2003), thus the SOC energy dissipation criterion is also met when measuring EEG phase reset. The exact physiological mechanisms of the conditional criteria of limited energy dissipation and preferred direction are likely related to the number and strength of connections and synaptic drives within and between clusters of neurons although detailed experimentation to test or quantify the physiological mechanisms have not as yet been conducted to the best of our knowledge.

Feigenbaum (1983) evaluated nonlinear systems in "criticality transitions" during the period of transition from quasi-periodic behavior to "chaos" and discovered that the expansion around this point is a $1/f^{\alpha}$ distribution. In other words the complex state at the border between predictable oscillatory

behavior and unpredictable chaos is the "Pink Noise" distribution called "one-over-f ". As pointed out by Bak (1997); Freeman et al (2003; 2006) and Buzsaki (2006) the brain approaches "chaos" followed by a transition to periods of phase locking. Understanding the details of the Feigenbaum's "Critical Point" during the transition from predictable behavior to "Chaos" is referred to as the Universality principle that was expanded by Haken (1983) to a general mathematical solution using a small set of "order parameters" to control the behavior of higher ordered systems. Once the value of the exponent in the $1/f^{\alpha}$ equation is known then the mathematics of SOC are more tractable (Rios and Zhang, 1999; Pikovsky et al, 2003). Future analyses of the 1st and 2nd derivatives of phase shift onset and offset may provide information about the energies involved in the transition from stability to "unstable phase dynamics" or when the brain briefly approaches "chaos".

4.3 – Long-Range Temporal and Spatial Correlations

As emphasized by Buzsaki (2006) and Freeman et al (2003; 2006) an attractive feature of SOC is its ability to describe complex systems behavior by simple power laws. The presence of the $1/f^{\alpha}$ distribution is a tell tale sign of self-organization and also measures the length of the correlation or "spatial and temporal memory effects" in the EEG signal. The slope of the log-log fit to the spectral distribution is an estimate of the temporal-range of the correlation in which the closer the slope approximates 1.0 then the stronger the long-range temporal correlations (Nikulin and Brismar, 2005; Stam and de Bruin, 2004). A possible spatial correlation is the differential rates of change in phase reset in the frontal lobes vs. the posterior cortical regions. For example, over the lifespan phase shift duration was flat in the short distance compartment but grew significantly (approx. 12 msec) in the long distance compartment (see fig. 7). The upward growth slope and the rapid growth spurts are nonlinear and can be fit by exponentials. This is important because in SOC models dynamic scaling is observed at equilibrium critical points where the power-law correlations in time are generated by long-range correlations in space (Bak et al, 1987; 1988).

In the present study we showed that the two components of phase reset (i.e., phase locking interval and phase shift duration) exhibit different coefficients in the $1/f^{\alpha}$ function where phase locking spectra exhibited a shorter temporal memory effect then the "unstable phase dynamics" which exhibited a longer-range scaling effect (see fig. 6 and Table III). The scale invariant properties of 1/f reflect the

temporal scaling of events that pre-date the occurrence of critical events and in the case of EEG phase locking there is reduced influence by past events and there is shorter spatial scaling. In contrast, phase shift duration is when phase stability is minimal and the brain approaches "chaos" with a period of high uncertainty and long-range temporal memory.

Another unique finding in this study is the observation of age dependent and ultra-slow changes in phase reset from infancy to adolescence (figs. 9 & 10). Growth spurts at age 9 and age 14 coincide with important behavioral developmental stages as hypothesized by Piaget (1975) and other developmental theorists (Case, 1985; 1987; Fischer, 1987; Fischer et al, 2007). These developmental theorists share a general theoretical assumption of the maturation of neural connections by genetic factors that are oscillatory with regular intervals. The findings in this study are consistent with these developmental models as well as identical and non-identical twin studies of the development of EEG coherence (van Baal, 2001; Van Beijsterveldt et al, 1998). The rhythmic order and cycles of phase reset are likely due to fundamental molecular processes involved in the production and elimination of synapses (Kandel, 2007; Thatcher et al, 1987; 1992; 1994; 1998). This is likely the case because EEG amplitude varies primarily as a function of the number, strength and phase locking of synaptic potentials (Niedermeyer and Lopes da Silva, 1995; Nunez, 1981; 1994). In the present study, environmental influences that effect the strength of cortical synaptic potentials are averaged over diversely different family experiences and different urban and rural environments. This fact tends to narrow the search for a causal link between slow rhythmic change in phase reset to slow rhythmic changes in the number of synaptic connections and less to short term rhythmic changes in the environmentally driven strength of synaptic connections.

4.3 – Temporal Boundaries of EEG Phase Reset

Shallace (1964); Allport (1968), Efron (1967; 1970a; 1970b) and others (Sanford, 1971; Varela, 1995) have shown a minimum perceptual frame from approximately 40 msec for auditory stimuli to 140 msec for visual stimuli required to temporally distinguish events as being successive in time. These studies as well as others show that learning-dependent changes in neural networks is not a continuous process but rather a discontinuous sequencing of narrow time windows (Thatcher and John, 1977; John, 2006). Event related desynchonization (ERD) studies show an approximate 200 msec delay between the onset of an event and a maximum amplitude reduction which extends until approximately 650 msec followed by a re-synchronization (ERS) of increasing EEG amplitude about 900 – 2000 msec (Klimesch

et al, 2007). The findings in this study may have relevance to perceptual frames and ERD by considering phase shift duration and phase locking intervals as elemental "atoms" or "quanta" that underlie perceptual frames and ERD. For example, figure 9 (Top) showed that phase reset is temporally bounded with a minimal phase shift duration of about 40 msec and a maximum phase shift duration of about 90 msec. Phase shift is followed by phase locking which, as seen in Figure 9 (Bottom), is also bounded from about 150 msec to about 800 msec with the most frequent phase locking intervals between 200 msec and 350 msec. Phase shift and phase locking are ongoing spontaneous processes that occur over widespread regions of the neocortex in resting conditions such as in the present study as well as during tasks. Whether or not the phase shift and phase locking are time locked to a task is irrelevant since "self-organizing criticality" is an ongoing background emergent process that on the average produces a 40 to 90 msec period of phase shift "uncertainty" or approximate "chaos" followed on the average by a 200 msec to 650 msec period of phase locking or "stability". This background process results in "blank" periods when large assemblies of neurons are in a phase reset mode (i.e., phase shift and phase locking). A type of "refractory" period is when phase locked neurons are unavailable for allocation by a different cluster of neurons at a different moment of time. Phase locking of a subset of a local cluster of neurons can result in a reduction in the amplitude of the surface EEG because phase locking occurs over long distances and thus reduces the size of the cluster of "idling" neurons by spatial differentiation. The findings in this study are consistent with models of event related desynchronization (ERD) in which the background phase reset as well as stimulus locked phase reset contribute to the ERD (Klimesch et al, 2007). This hypothesis of linking phase reset during the background spontaneous EEG to ERD provides a new definition of the term "desynchronization" used to describe event related desynchronization (ERD) in that desynchronization is actually "spatially differentiated phase locking" or "micro bonding" as the underlying mechanism that removes available neurons from the "idling" population of neurons resulting in a reduction in the average amplitude of the post-stimulus EEG.

4.4 – Phase Reset in Local versus Distant Connection Systems

The short inter-electrode distance exhibited stronger developmental changes in the mean phase locking interval than the long inter-electrode distance, especially in the posterior-to-anterior direction. The short inter-electrode distance also exhibited larger growth spurts in phase locking intervals than the long inter-electrode distance connections (see fig 8). In contrast to phase locking, the mean phase shift

duration declined in the local frontal connections while it increased in the long inter-electrode distance (see fig. 7 & Table IV). This showed that local connections exhibited shorter periods of unstable phase dynamics than the distant connections. In general, long distance connections exhibited longer phase shift durations (i.e., more "instability") than local connections (see fig. 7). The finding that phase locking intervals only modestly increased with age in the long distance systems but strongly increased in the local connections indicates that maturation is dominated more by local phase locking in comparison to the long distances where there is a slower refinement process involved in the development of the long distance system.

Previous studies have used two compartment models of EEG coherence in which the number of connections and the strength of connections influence the magnitude of coherence (Nunez, 1981; Thatcher et al, 1986; 1998; 2007; McAlaster, 1992; Hanlon and Thatcher, 1999; Van Beijsterveldt et al 1998; van Baal et al, 2001). According to these models, a positive correlation between coherence and phase locking is expected since coherence is a measure of phase consistency (Otnes and Enochson, 1978; Bendat and Piersol, 1980). Also, one would expect a negative correlation between phase shift duration and coherence since phase shift duration is related to unpredictability and reduced phase stability. This study supports the two compartment connection models by demonstrating a significant difference between local vs. distant connections with a positive correlation between phase locking intervals ("stability") and coherence and a negative correlation to phase shift duration ("unstable phase dynamics"), especially in the local or short inter-electrode pairs. The findings in this study are also consistent with EEG coherence studies (Thatcher et al, 1986; 1998; 2007; McAlaster, 1992; van Ball et al, 2001; Van Beijsterveldt et al, 1998) which hypothesize that fluctuations of EEG coherence during development are due largely to fluctuations in the number of cortical synaptic connections.

A simple and unifying mathematical model that links the development of the number and/or density of synaptic connections to EEG coherence (Thatcher, 1994; Thatcher et al, 2007) and to the two components of phase reset, i.e., "Unstability" (phase shift duration) and "Stability" (phase locking interval) is shown in equation 11:

$$\boldsymbol{N_{ij} \Rightarrow K \frac{S_{ij}}{C_{ij}}} \qquad (11)$$

Where N_{ij} = the number and/or density of local synaptic connections in a matrix, K_{ij} = a proportionality constant, S_{ij} = "Stability" defined as the average phase locking interval and C_{ij} =

"Unstable phase dynamics" defined as the average phase shift duration. S_{ij}/C_{ij} is the stability to chaos ratio where the number and/or density of synaptic connections is inversely related to the tendency toward "chaos" and directly related to stability. During short periods of time the relationship on each side of the equals sign is likely a two-way relationship, however, the arrow symbol $\Rightarrow$ represents the slow developmental trend over a lifespan which gives greater weight to the relationship between the number of synaptic connections as influencing "unstability" and "stability" rather than the reverse direction. Certainly, phase locking or phase synchrony is important for learning, perception and memory and thus the environment must be an important factor in determining the number of connections between different brain regions as well as the dynamics of phase reset. However, the oscillations and growth spurts in phase reset are averages over the lifespan from environmentally diverse subjects and thus, there is greater weight given to the number and/or density of synaptic connections as determining the balance between "unstable phase dynamics" and "stability" over the maturation period from infancy to adolescence. That is, as the number of synaptic connections increases during maturation then phase stability increases and the duration of phase shift "uncertainty" decreases. It is relevant that ecological models of cooperation, competition, independence and predator/prey involving nonlinear regulation of synaptogenesis have been applied to measures of human cortical development (Thatcher, 1994; 1998; Edelman, 1987). The findings generally support SOC epigenetic models of human brain development where growth spurts are punctuations or "unstable phase dynamics" within periods of stability and the underlying 1/f dynamics represent long-range temporal and spatial correlations. The linkage of the number and/or density of synaptic connections to SOC suggests that packing density and the number of synaptic connections may be critical order parameters that determine some of the dynamics of cortico-cortical coupling during human development.

4.5 – Differences in the anterior-to-posterior versus the posterior-to-anterior direction

The strongest difference between the anterior-to-posterior vs. the posterior-to-anterior direction of electrode placement are the phase shift duration differences in the short inter-electrode distances. The development of EEG phase shift duration in the anterior-to-posterior direction exhibited a negative slope with age, whereas the short distances exhibited a positive slope with age in the posterior-to-anterior direction. The development of the magnitude of phase locking intervals were also different in the short inter-electrode distance in the anterior-to-posterior vs. the posterior-to-anterior directions. The directional difference in development of phase shift duration and phase locking intervals can be

explained by a simple and unifying concept, similar to that to explain EEG coherence and EEG phase differences in local and distant connections (Thatcher et al, 1986; 1998). The unifying concept is that the findings are consistent with a differential preference for packing density in local brain regions with greater packing density in occipital brain regions in comparison to the frontal lobes. For example, the occipital brain regions have the highest neural packing density and the frontal lobes have the lowest packing density (Blinkov and Glezer, 1968; Carpender and Sutin, 1983). The number of connections is related to the packing density by virtue of the available area on dendrites for synaptogenesis (Purves, 1988). Although high packing density can result in shorter dendrites, nonetheless, with more neurons there are more synaptic connections. This conclusion is consistent with equation 11, where reduced connections are related to increased periods of "unstable phase dynamics" and increased number of connections is related to longer synchronization intervals and shorter periods of unstable dynamics.

As seen in figures 7 and 9, the mean and mode of phase shift duration is shorter in the frontal lobes than in posterior regions at the same interelectrode distance (i.e., 6 cm). Previous studies have shown that the shorter the phase difference between local frontal regions then the higher is the I.Q. (Thatcher et al, 2005). The interpretation offered for shorter phase delays and higher I.Q. is that the faster that the frontal lobes orchestrate the resources of the posterior neocortex then the higher the I.Q. (Thatcher et al, 2005). Because the same subjects are used in the present study as in the earlier Thatcher et al (2005) study the present findings are consistent with this interpretation and extend the earlier findings to implicate more rapid phase shift as a component of shorter phase delays.

Another finding of interest was that the local or short inter-electrode distances exhibited larger growth spurts (age 9 and age 14) in the posterior-to-anterior direction than in the anterior-to-posterior direction. The occipital-parietal growth spurts at age 9 and 14 may correspond to the development of visual-spatial information processing as well as more abstract aspects of language and cognitive development which occur during these ages (Case, 1985; 1987; Fischer, 1983; 1987). The fact that the largest growth spurts occurred in the phase locking interval and not in phase shift duration suggests that the developmental changes during these age periods involve increased network stability and increased integration in contrast to an increased tendency to "chaos".

4.6 – Nonlinear Oscillations in SOC and Growth Spurts

The frequency spectrum of the development of phase shift duration and phase locking intervals showed significant ultraslow oscillations over the lifespan from infancy to adolescence. The mean

frequency of oscillations were different in the anterior-to-posterior and posterior-to-anterior directions and for different inter-electrode distances but they were similar for left and right hemispheres (see figs. 9 & 10 and tables VII & VIII). The strongest spectral magnitudes in the development of phase shift duration and phase locking were repetitive cycles at wavelengths between 8 years and 2 years. The highest frequency of oscillations were approximately 1 year wavelengths and the higher frequency oscillations exhibited the lowest power. Additional studies, such as identical and non-identical twin studies, can test the genetic contributions to the development of EEG phase reset. We have found that phase reset per second while correlated as expected is often unrevealing and masks some of the underlying dynamics because of the short time frame of phase shift duration and the long time frame of phase locking. It is necessary to measure both phase shift duration and the phase locking interval in order to understand phase resets per second. Mathematical neural network models of the development of EEG phase reset can test developmental hypotheses and animal studies can be used to further evaluate the genetics and molecular biology of EEG phase reset.

5.0 – References

Allport, D.A. (1968). Phenomenal simultaneity and perceptual moment hypotheses. Br. J. Psychol., 59: 395–406.

Bak, P., Tang, C. and Wisenfeld, K. (1987). Self-organized criticality: An explanation of 1/f noise. Physical Rev. Letters, 59(4), 381-384.

Bak, P., Tang, C. and Wisenfeld, K. (1988). Self-organized criticality. Physical Rev. A. 38(1): 364-374.

Bak, P. (1996). How Nature Works: The science of Self-Organized Criticality. Springer-Verlag, New York.

Berryman, A. A. (1981). *Population systems: A general introduction.* New York: Plenum Press.

Beggs, J.M. and Plenz, D. (2003). Neuronal avalanches in neocortical circuits. J. Neurosci., 23: 11167-11177.

Bendat, J. S. & Piersol, A. G. (1980). *Engineering applications of correlation and* spectral analysis. New York: John Wiley & Sons.

Blinkov, S. M. and Glezer, I., (1968). The Human Brain in Figures and Tables: A Quantitative Handbook, Basic Books, Inc., Publisher Plenum Press.

Bloomfield, P. (2000). Fourier Analysis of Time Series: An Introduction, John Wiley & Sons, New York.

Breakspear, M. and Terry, J.R. (2002a). Detection and description of non-linear interdependence in normal multichannel human EEG data. Clin. Neurophysiol., 113(5): 735-753.

Breakspear, M. and Terry, J.R. (2002b). Nonlinear interdependence in neural systems: motivation, theory and relevance. Int. J. Neurosci., 112(10): 1263-1284.

Breakspear, M. (2002). Nonlinear phase desynchronization in human electroencephalographic data. Hum. Brain Mapp., 15(3): 175-198.

Breakspear, M. (2004). Dynamic connectivity in neural systems: theoretical and empirical considerations. Neuroinformatics, 2(2): 205-226.

Breakspear, M. and Williams, L.M. (2004). A novel method for the topographic analysis of neural activity reveals formation and dissolution of 'dynamic cell assemblies'. J. Computational Neurosci., 16, 49-68.

Buzsaki, G. and Draguhn, A. (2004). Neuronal oscillations in cortical networks. Science, 304(5679): 1926-1929.

Buzsaki, G. (2006). Rhythms of the Brain, Oxford Univ. Press, New York.

Bruns, A. (2004). Fourier, Hilbert and wavelet-based signal analysis: are they really different approaches? J. Neurosci. Methods, 137(2): 321-332.

Carpenter, M.B. and Sutin, J. (1983). Human Neuroanatomy, 8th edition, Williams and Wilkins, Baltimore, Maryland.

Case, R. (1985). Intellectual development: Birth to adulthood. Academic Press, New York.

Case, R. (1987). The structure and process of intellectual development. International Journal of Psychology, 22, 571-607.

Chavez, M., Le Van Quyen, M., Navarro, V., Baulac, M. and Martinerie, J. (2003). Spatio-temporal dynamics prior to neocortical seizures: amplitude versus phase couplings. IEEE Trans. Biomed. Eng. 50(5): 571-583.

Chialvo, D.R. and Bak, P. (1999). Learning from mistakes. Neuroscience, 90:1137-1148.

Cooper R, Winter AL, Crow HJ and Walter WG. (1965). Comparison of subcortical, cortical and scalp activity using chronically indwelling electrodes in man. Electroencpehalogr Clin Neurophysiol. 18:217-222.

Cosmelli, D., David, O., Lachaux, J.P., Martinerie, J., Garnero, L., Renault, B. and Varela, F. (2004). Waves of consciousness: ongoing cortical patterns during binocular rivalry. Neuroimage, 23(1): 128-140.

Damasio, A.R. (1989). Time-locked multiregional retroactivation: A systems-level proposal for the neural substrates of recall and recognition. Cognition, 33: 25-62.

Davidson, J. and Schuster, H.G. (2000). $1/f^{\alpha}$ noise from self-organized critical models with uniform driving. Physical Review E, 62(5), 6111-6115.

Edelman, G.M (1987). Neural Darwinism: The Theory of Neuronal Group Selection. New York, Basic.

Efron, E. (1967). The duration of the present. Annals of the New York Acad. Sci., 138: 713-729.

Efron, E. (1970a). The relationship between the duration of a stimulus and the duration of a perception. Neuropsychologia, 8: 37-55.

Efron, E. (1970b). The minimum duration of a perception. Neuropsychologia, 8: 57–63.

Essl, M. and Rappelsberger, P. (1998). EEG coherence and refernce signals: experimental results and mathematical explanations. Med. Biol. Eng. Comput., 36: 399-406.

Feigenbaum, M.J. (1983). Universal behavior in nonlinear systems. Physica, 7D: 16-19.

Fischer, K.W., Rose, T.L. and Rose, S.P. (2007). Growth cycles of mind and brain: Analyzing developmental pathways of learning disorders. In K.W. Fischer, J. Holmes-Bernstein and M. H. Immordino-Yang (Eds.), Mind, Brain and Education in Reading Disorders. Cambridge Univ. Press, MA.

Fischer, K.W. (1987). Relations between brain and cognitive development. Child Development, 57, 623-632.

Freeman, W.J. (2003). Evidence from human scalp electroencephalograms of global chaotic itinerancy. Chaos, 13(3): 1067- 1077.

Freeman, W.J. and Baird, B. (1987). Relation of olfactory EEG to behavior: Spatial analysis. Behav. Neurosci., 101: 393-408.

Freeman w.J. and Rogers, L.J. (2002). Fine temporal resolution of analytic phase reveals episodic synchronization by state transitions in gamma EEGs. J. Neurophysiol, 87(2): 937-945.

Freeman, W.J., Burke, B.C. and Homes, M.D. (2003). Aperiodic phase re-setting in scalp EEG of beta-gamma oscillations by state transitions at alpha-theta rates. Hum Brain Mapp. 19(4):248-272.

Freeman, W.J., Homes, M.D., West, G.A. and Vanhatlo, S. (2006). Fine spatiotemporal structure of phase in human intracranial EEG. Clin Neurophysiol. 117(6):1228-1243.

Granger, C.W.J. and Hatanka, M. (1964). Spectral Analysis of Economic Time Series, Princeton University Press, New Jersey.

Hanlon, H. W., Thatcher, R. W. & Cline, M. J. (1999). Gender differences in the development of EEG coherence in normal children. *Developmental* Neuropsychology, *16* (3), 479-506.

Haken, H. 1983. “Synergetics, An Introduction”, Springer-Verlag, Berlin.

Jensen, O., and Lisman, J.E. (1998). An oscillatory short-term memory buffer model can account for data on the Sternberg task. J Neurosci. 18(24):10688-10699.

John, E.R. (1968), Mechanisms of Memory. Academic Press, New York.

John, E.R. (2002). The neurophysics of consciousness. Brain Res Brain Res Rev. 39(1):1-28.

John, E.R. (2005). From synchronous neural discharges to subjective awareness? Progress in Brain Research, Vol. 150: 143-171.

Kahana, M.J. (2006). The cognitive correlates of human brain oscillations. J. Neurosci., 26:1669-1672.

Kamiński, M., Blinowska, K.J., and Szelenberger, W. (1997). Topographic analysis of coherence and propagation of EEG activity during sleep wakefulness. EEG and Clin. Neurophysiol., 102: 216-227.

Kandel, E. R. (2007). In Search of Memory: The Emergence of a New Science of Mind. John Wiley & Sons, New York.

Kirschfeld, K. (2005). The physical basis of alpha waves in the electroencephalogram and the origin of the "Berger effect"., Biol. Cybem., 92(3):177-185.

Klimesch, W., Sauseng, P., Hanslmayr, S., Gruber, W. and Freunberger, R. (200&). Neurosci. and Biobehav. Rev., 31: 1003-1016.

Lachaux, J.-P., Rodriguez, E., Martinerie, J. anjd Varela, F.J. (1999). Measuring phase locking in brain signals. Hum. Brain Mapp. 8(4): 194-208.

Lachaux, J.-P., Rodriguez, E., Le Van Quyen, M., Lutz, A., Martinerie, J., Varela, F.J. (2000) Studying single-trials of phase synchronous activity in the brain. Int. J. Bifuc. Chaos, 10(10): 2429-2439.

Le Van Quyen, M., Foucher, J., Lachaux, J.-P., Rodriguez, E., Lutz, A., Martinerie, J. and Varela, F.J. (2001a). Comparison of Hilbert transform and wavelet methods for the analysis of neuronal locking. J. Neurosci. Methods, 111(2): 83-89.

Le Van Quyen, M., Martinerie, J., Navarro, V. and Varela, F.J. (2001b). Characterizing neurodynamic changes before seizures. J. Clin. Neurophysiol., 18(3): 191-208.

Le Van Quyen, M. (2003). Disentangling the dynamic core: A research program for a neurodynamics at the large-scale. Biol. Res., 36: 67-88.

Linkenkaer-Hansen, KI., Nikouline, V.V., Palva, J.M and Ilmoniemi, R.J. (2001). Long-range temporal correlations and scaling behavior in human brain oscillations. J. Neurosci. 21:1370-1377.

Lopes Da Silva, F.H. (1995). Dynamic of Electrical Activity of the Brain, Networks, and and Modulating Systems. In: P. Nunez, ed., *Neocortical Dynamics and Human EEG Rhythms*, 249-271.

Lopes Da Silva, F.H. and Pijn, J.P. (1995). Handbook of Brain Theory and Neural Networks. MIT Press, Arbib, Cambridge.

McAlaster, R. (1992). Postnatal cerebral maturation in Down's syndrome children: a developmental EEG coherence study, Int. J. Neurosci., 65(1-4): 221-2237.

McCartney, H., Johnson, A.D., Weil, Z.M. and Givens, B. (2004). Theta reset produces optimal conditions for long-term potentiation. Hippocampus, 14(6):684-697.

Netoff, T.I. and Schiff, S.J. (2002). Decreased neuronal synchronization during experimental seizures. J. Neurosci., 22(16): 7297-7307.

Niedermeyer, E. and Lopes da Silva, F. (1994). Electroencephalograph: Basic Principles, Clinical Applications and Related Fields, Wilkins and Williamson, Baltimore, Md.

Nikulin, V.V. and Brismar, T. (2004). Long-range temporal correlations in alpha and beta oscillations: effect of arousal level and test-retest reliability. Clin. Neurophysiol., 115: 1896-1908.

Nikulin, V.V. and Brismar, T. (2005). Long-range temporal correlations in electroencephalographic oscillations: Relation to topography, frequency band, age and gender. Neurosci., 130: 549-558.

Nunez, P. (1981). Electrical Fields of the Brain. Oxford University Press, New York.

Nunez, P. (1994). Neocortical Dynamics and Human EEG Rhythms, Oxford University Press, New York.

Oppenheim, A.V. and Schafer, R.W. (1975). Digital Signal Processing, Printice-Hall, London.

Otnes, R.K. and Enochson, L. (1978). Applied Time Series Analysis, John Wiley & Sons, New York.

Parish, L.M., Worrell, G.A., Cranstun, S.D., Stead, S.M., Pennell, P. and Litt, B. (2004). Long-range temporal correlations in epileptogenic and non-epileptogenic human hippocampus. Neurosci., 125: 1068-1076.

Piaget, J. (1975). Biology and Knowledge (2nd ed.). University of Chicago Press, Chicago.

Pikovsky, A., Rosenblum, M. and Kurths, J. (2003). Synchronization: A universal concept in nonlinear sciences. Cambridge Univ. Press, New York.

Purves, D. (1988). *Body and brain: A trophic theory of neural connections.* Boston: Harvard University Press.

Rappelsberger, P. (1989). The reference problem and mapping of coherence: A simulation study. Brain Topog. 2(1/2): 63-72.

Rios, L.P. and Zang, Y.C. (1999). Universal 1/f noise from dissipative self-organized criticality models. Phys. Rev. Let., 82(3): 472-475.

Rizzuto, D.S., Madsen, J.R., Bromfield, E.B., Schultz-Bonhage, A., Seelig, D., Aschenbrenner-Scheibe, R. and Kahana, M.J. (2003). Reset of human neocortical oscillations during a working memory task. Proc Natl Acad Sci U S A. 100(13):7931-7936.

Roelfsmema, P.R., Engel, A.K., Konig, P. and Singer, W. (1997). Visuomotor integration is associated with zero time-lag synchronization among cortical areas. Nature, 385(6612): 157-161.

Rudrauf, D., Douiri, A., Kovach, C., Lachaux, J.P., Cosmelli, D., Chavez, A., Renault, B., Marttinerie, J. and Le Van Quyen, M. (2006). Frequency flows and the time-frequency dynamics of multivariate phase synchronization in brain signals. Neuroimage, 31: 209-227.

Savitzky, A. and Golay, M.J.E. (1964). Smoothing and differentiation of data by simplified least squares procedures, Analytic Chemistry, 36: 1627-1639.

Sanford, A.J. (1971). A periodic basis for perception and action. In: Biological Rhythms and Human Performance. W.P. Colquhoun (Ed.). New York, Academic Press.

Shallice, T. (1964). The detection of change and the perceptual moment hypothesis. British Journal of Stat. Psychol., 17: 113-135.

Stam, C.J. and de Bruin, E.A. (2004). Scale-free dynamics of global functional connectivity in the human brain. Hum. Brain Map. 22:97-109.

Stam, C.J. and de Bruin, E.A. (2004). Scale-free dynamics of global functional connectivity in the human brain. Hum. Brain Mapping, 22:97-109.

Tallon-Baudry, C., Bertrand, O., and Fischer, C. (2001). Oscillatory locking between human extrastriate areas during visual short-term memory maintenance. J. Neurosci., 21(20): RC177.

Tass, P.A. (1997). Phase Resetting in Medicine and Biology, Springer-Verlag, Berlin.

Tass, p.A., Rosenblum, M.G., Weule, J., Kurths, J., Pikovsky, A., Volkmann, J. aSchnitzler, A. and Freund, H.J. (1998). Detection of n:m phase locking from nosy data: application to magnetoencephalography. Phys. Rev. Lett., 81(15): 3291-3294.

Tesche, C.D. and Karhu, J. (2000). Theta oscillations index human hippocampal activation during a working memory task. Proc Natl Acad Sci U S A. 18;97(2):919-924.

Thatcher, R.W., Krause, P and Hrybyk, M. (1986). Corticocortical Association Fibers and EEG Coherence: A Two Compartmental Model. Electroencephalog. Clinical Neurophysiol., 64: 123 – 143.

Thatcher, R.W., Walker, R.A. and Guidice, S. (1987). Human cerebral hemispheres develop at different rates and ages. Science, 236: 1110-1113.

Thatcher, R.W. (1992). Cyclic cortical reorganization during early childhood. Brain and Cognition, 20: 24-50.

Thatcher, R.W. (1994). Psychopathology of Early Frontal Lobe Damage: Dependence on Cycles of Postnatal Development. Developmental Pathology, 6: 565-596.

Thatcher, R. W., Biver, C., McAlaster, R and Salazar, A.M. (1998). Biophysical linkage between MRI and EEG coherence in traumatic brain injury. NeuroImage, 8(4), 307-326.

Thatcher, R.W. (1998). A predator-prey model of human cerebral development. In: K. Newell and P. Molenaar Editors, Dynamical Systems in Development, L. Erlbaum Assoc, New Jersey.

Thatcher, R.W., North, D., and Biver, C. (2005). EEG and Intelligence: Univariate and Multivariate Comparisons Between EEG Coherence, EEG Phase Delay and Power. Clinical Neurophysiology, 116(9):2129-2141.

Thatcher, R.W., North, N. and Biver, C.J. (2007). Development of cortical connections using EEG coherence and phase (submitted for publication).

Thompson, J.M.T. and Stewart, H.B. (1986). Nonlinear Dynamics and Chaos. John Wiley & Sons, New York.

Vaadia, E., Haalman, L., Abeles, M., Bergman, H., Prut, Y., Slovin, H. and Aertsen, A. (1995). Dynamics of neuronal interactions in monkey cortex in relation to behavior events. Nature, 373(6514): 515-518.

Varela, F.J. (1995). Resonant cell assemblies: a new approach to cognitive functions and neuronal locking. Biol. Res., 28(1): 81-95.

Varela, F.J., Lachaux, J.-P., Rodriguez, E., and Martinerie, J. (2001). The brainweb: phase synchronization and large-scale integration. Nat. Rev., Neurosci., 2(4): 229-239.

van Baal, G.C., Boomsma, D.I. and de Geus, E.J. (2001). Longitudinal genetic analysis of EEG coherence in young twins. Behav. Genet., 31(6):637-651.

Van Beijsterveldt, C.E., Molenaar, P.C., de Geus, E.J. and Boomsma, D.I. (1998). Genetic and environmental influences on EEG coherence. Behav. Genet., 28(6): 443-453.

Watts, D.J. and Strogatz, S.H. (1998). Collective dynamics of "small-world" networks. Nature, 393:440-442.

Winfree, A.T. (1980). The Geometry of Biological Time. Springer, New York.